



Original article

Functional assessment of microbial superoxide dismutase isozymes suggests a differential role for each isozyme

Hastyar Najmuldeen^{a,b}, Rashed Alghamdi^a, Fayez Alghofaili^{a,c}, Hasan Yesilkaya^{a,*}^a Department of Infection, Immunity and Inflammation, University of Leicester, University Road, Leicester LE1 9HN, UK^b Department of Biology, College of Science, University of Sulaimani, Sulaymaniyah, Kurdistan Region, Iraq^c Department of Biology, College of Science, Majmaah University, Majmaah 11952, Saudi Arabia

ARTICLE INFO

Keywords:

Superoxide dismutase

Isozymes

Oxidative stress resistance

Klebsiella pneumoniae

Biofilm

Mucoviscosity

Cell morphology

Lung infection

Persistence

ABSTRACT

Microbes can have multiple enzymes that are able to catalyse the same enzymatic reactions but may differ in structure. These are known as isozymes. It is assumed that isozymes have the same functional role for cells. Contrary to this assumption, we hypothesised that isozymes can confer different functions for microbial cells despite catalysing the same reactions. To test this hypothesis, we studied the role of superoxide dismutases (SOD) in *Klebsiella pneumoniae*, the causative agent of several nosocomial and community-acquired infections, in infection relevant assays. SODs are responsible for detoxification of toxic superoxide radicals. *K. pneumoniae* genome contains three superoxide dismutase genes, *sodA*, *sodB*, and *sodC* coding for Mn-, Fe- and CuZn- co-factored SODs, respectively. By creating and testing single, double, and triple SOD mutants, we investigated the regulatory interactions among SOD and determined the role of each isozyme in oxidative stress resistance, biofilm formation, cell morphology, metabolism, and *in vivo* colonization and persistence. Our results demonstrate that SOD isozymes in *K. pneumoniae* have unique roles beyond oxidative stress resistance, and there is a regulatory interplay among SODs.

1. Introduction

Reactive oxygen species (ROS) are harmful derivatives of oxygen including superoxide ($O_2^{\cdot-}$), hydrogen peroxide (H_2O_2), and hydroxyl radical ($\cdot OH$). ROS are more chemically reactive than O_2 and are formed either by one-electron reduction of molecular oxygen, through dismutation of $O_2^{\cdot-}$, i.e. H_2O_2 , or from electron exchange between $O_2^{\cdot-}$ and H_2O_2 via the Haber–Weiss reaction, or generated by the reduction of H_2O_2 by the Fenton reaction, i.e. $\cdot OH$ [1]. ROS are harmful to various biomolecules, for instance, $O_2^{\cdot-}$ and H_2O_2 damage proteins, whereas $\cdot OH$ targets DNA [1,2].

Superoxide is capable of inflicting overwhelming cell damage as its direct interaction with specific cellular constituents provides substrates for the Haber–Weiss reaction [1]. Resulting hydroxyl radical production subsequently damages molecules that are superoxide resistant. To counter the adverse effects of superoxide toxicity, most bacteria that survive in oxygenated habitats encode an enzyme called superoxide dismutase (SOD), which converts superoxide radical to the less toxic H_2O_2 and water. When present, the number of SOD isozymes in microbes can generally vary from one to three including cytoplasmic Mn-SOD (encoded by *sodA*), the Fe-SOD (encoded by *sodB*), and periplasmic

Cu/Zn-SOD (encoded by *sodC*) [3,4]. The multiplicity of SOD isozymes reflects the importance of $O_2^{\cdot-}$ removal. The first strong evidence that *in vivo* superoxide is harmful to the bacterial cell was demonstrated by generating and testing *Escherichia coli* mutants devoid of cytoplasmic SOD in limited *in vitro* assays [5]. This double *sodA::sodB* mutant was able to grow in the presence of oxygen providing that branched-chain, sulphur containing, and aromatic amino acids were added. The mutant also grew more slowly in rich medium, which also needed the addition of fermentable carbon, and showed a higher rate of spontaneous mutagenesis [6,7].

As far as it is known all SOD isozymes catalyse the same enzymic reaction. It is not known why there are multiple enzymes for the same substrate, however. The main hypothesis as to why multiple SOD isozymes evolved has been linked to the increase in the concentration of atmospheric and oceanic oxygen levels, and the impact of this event on the metal availability [8]. There are several additional specific hypotheses that attempt to explain the multiplicity of SOD isozymes. The first view suggests that the variation in the concentration of metal ions in different compartments of microbial cells [9], gave rise to the evolution of multiple SOD isozymes so that the efficient posttranslational control of SOD metalloenzymes could occur [8]. Another hypothesis

* Corresponding author.

E-mail address: hy3@le.ac.uk (H. Yesilkaya).<https://doi.org/10.1016/j.freeradbiomed.2019.01.018>

Received 20 September 2018; Received in revised form 6 December 2018; Accepted 14 January 2019

Available online 15 January 2019

0891-5849/© 2019 The Authors. Published by Elsevier Inc. This is an open access article under the CC BY-NC-ND license (<http://creativecommons.org/licenses/by-nc-nd/4.0/>).

links the diversity of SOD enzymes to the inability of $O_2^{\cdot-}$ to cross cell membranes and necessity to remove $O_2^{\cdot-}$ in the location where it is produced [10]. This view has been supported by previous studies in *Legionella pneumophila*, which indicated that periplasmic Cu/Zn-SOD cannot replace the absence of cytoplasmic Fe-SOD [11], nor that cytosolic SODs could replace the function of periplasmic Cu/Zn-SOD [12]. The expression of individual *sod* can also differ. The reason for this observation is not known in detail but was linked to the promoter structure [13,14]. For example, *sodB* is constitutively expressed when bacteria grow under anaerobic and aerobic growth conditions, whereas *sodA* is expressed in response to an anaerobic challenge and high oxygen concentration [5,11].

In order to understand the evolutionary benefit of having multiple SOD isozymes, it is a prerequisite, first, to systematically characterise the function of each SODs. Previous studies investigated the role of selected SODs by analysis of isogenic mutants in limited experimental settings in selected microbial species [5,15]. These studies often under-appreciated the regulatory interactions among SOD isozymes and the wider roles of SOD other than their contribution to the removal of $O_2^{\cdot-}$ toxicity. Hence, we have the only limited view of SOD isozymes function in bacteria. To fill the gap in knowledge, we functionally characterised the role of SOD enzymes in *K.pneumoniae*, which has the homologues of *sodA*, *sodB* and *sodC*. To attribute a function to each SOD and to understand the inter-regulatory interactions among SOD isozymes, we created single, double and triple SOD isogenic mutants, and characterised them using *in vitro* and *in vivo* assays relevant to infection. Our results show that in addition to the removal of superoxide radicals, SODs have a major influence on metabolism and are fundamental for *K.pneumoniae* virulence and host colonization.

2. Materials and methods

2.1. Bacterial strains, and growth conditions

Klebsiella pneumoniae KR3167 isolate was kindly provided by Dr Kumar Rajakumar, University of Leicester, UK. Routinely, *K. pneumoniae* strains were grown at 37 °C in LB broth or agar, and when required, supplemented with kanamycin (30 µg ml⁻¹), apramycin (30 µg ml⁻¹), ampicillin (1200 µg ml⁻¹), 6% (w/v) sucrose, or 60 µM paraquat (methyl viologen dichloride hydrate), which generates superoxide. In addition, *K. pneumoniae* was also grown in M9- and milk broth [5,16–18]. Growth was initiated by using a standard inoculum containing approximately 10⁵ CFU ml⁻¹ prepared from early exponential phase culture (OD₆₀₀ of 0.1), and media inoculated at a 1:100 ratio. Bacterial growth was maintained on shaker incubator (200 rpm) at 37 °C and the growth was determined by measuring an increase in absorbance or by viable count [19].

2.2. Construction of unmarked SOD mutants using the Lambda Red recombination system

Mutagenesis methods used in this study relied on the construction of mutagenized recombinant DNA by splicing overlap extension using the primers listed in Supp. Table 1. The transformation of mutagenized constructs into the recipient *K. pneumoniae* KR3167 strain that contained pKOBEG-Apra was done as described previously [17,20]. Once the marked mutant was constructed, it was cured of pKOBEG-Apra, and antibiotic cassette using pFLP2 (Supp. Table 2) [18,21]. Finally, pFLP2 was cured by incubating the mutant strain in the presence of 6% (w/v) sucrose at 37 °C [16,18]. The same method was used to construct *cis*-complementation in *sodA*, *sodB* and *sodC* mutants. DNA sequencing was used for final confirmation of unmarked mutants.

2.3. RNA extraction, cDNA synthesis, and quantitative reverse transcriptase real-time PCR (qRT-PCR)

RNA extraction was performed from mid-exponential phase cultures using Trizol (TRI) (Sigma-Aldrich) extraction method as previously described [22–24]. All RNA samples were treated with Turbo DNA free kit (Ambion). Then, first-strand cDNA was synthesised from 1 µg DNase treated RNA sample using SuperScript™ III Reverse Transcriptase kit, and random primers (Invitrogen). Transcriptional levels of *sod* genes were determined using gene-specific primers (Supp. Table 3) and normalized to the transcriptional level of *rpoD*, which was amplified in parallel. Data were analysed by the comparative threshold method (2^{-ΔΔCT}) [25]. Differences in expression of two-fold or greater relative to control were considered as significant.

2.4. Enzyme activity assays

The SOD activity in *K. pneumoniae* strains was measured using a commercial kit (SOD Assay Kit-WST, Sigma-Aldrich). β-galactosidase activity was assayed qualitatively and quantitatively. Qualitative β-galactosidase activity relies on the conversion of soluble chromogenic substrate X-Gal (5-bromo-4-chloro-3-indolyl-β-D-galactopyranoside) to an insoluble blue compound by the action of β-galactosidase [26]. For quantitative β-galactosidase activity, 2-Nitrophenyl β-D-galactopyranoside was used as previously described [27]. Hydrogen peroxide determination used PeroxiDirect™ kit (Sigma-Aldrich).

2.5. Determination of capsule production

The capsular polysaccharides (CPS) were extracted as described previously [28]. Briefly, 1000 µl of overnight bacterial culture was mixed with 200 µl of 1% (v/v) Zwittergent 3–14 detergent (Sigma-Aldrich, UK) in 100 mM citric acid (pH 2.0). The bacterial cells were pelleted after incubation at 50 °C for 20 min. A 300 µl supernatant was taken to a fresh tube, and 1200 µl of absolute ethanol was added to the final concentration of 80% (v/v). For CPS precipitation, the mixture was kept at 4 °C for 20 min, and pelleted at 12,000 × g for 5 min. Finally, the supernatant was discarded and the pellet was dissolved in 200 µl of de-ionized water [29,30]. Uronic acid concentration was quantified in extracted CPS samples, using previously described carbazole assay [28]. Then, the concentration of glucuronic acid in the samples was calculated using a standard curve prepared with the known glucuronic acid concentrations. Finally, the concentration of CPS for each strain was expressed as µg of uronic acid per Log₁₀ 9 CFU [29,31].

3. Biofilm assay using crystal violet staining method

Crystal violet staining was used for quantitative measurement of biofilm production after 24 h incubation at 37 °C as previously described [32]. To rule out that difference in biofilm formation among the strains was not due to the growth properties, the bacterial numbers in culture supernatant and biofilm former cells were also quantified. Planktonic cells were aseptically transferred into a new 12-well flat-bottomed plate, and the attached cells were washed twice by LB broth medium. To remove adherent cells from the plate, 1 ml PBS was added, and the cells were detached by cell scraper (Biologix) and by pipetting. Viable cells in the planktonic and biofilm phases were determined by viable plate count [33]. As a further confirmation, trimethyl tetrazolium chloride (TTC) was used to determine metabolically active cells in undistracted biofilm matrix [34,35]. The principle of this test is based on the reduction of trimethyl tetrazolium chloride (TTC) to insoluble formazan crystals, which is visible as a red deposition in the cell [34]. Finally, to test the effect of *sod* mutation on hydrophobicity and surface charge of *K. pneumoniae*, Microbial Adhesion to Solvent (MATS) test was conducted as previously described [36].

3.1. Microscopic analysis

To visualize the structure of biofilms, 3 ml of inoculated LB medium (1:100) was transferred into 12-well flat bottom polystyrene microplate. Then, 2/3 of the length of sterilized cover slides were vertically merged into the inoculated medium and incubated at 37 °C for 24 h. Subsequently, the cover slides were washed twice in PBS, allowed to dry at room temperature, stained with 0.5% (v/v) crystal violet for 1 min, and washed twice in PBS. The stained cover slides were fixed on slides and examined under a light microscope (Nikon Labophot)

Electron microscopy analysis of bacterial morphology was performed in collaboration with Electron Microscope Facility, Core Biotechnology Services, University of Leicester. For scanning electron microscopy, LB medium was inoculated (1:100) with wild type and mutant strains, and distributed into two 12-well microplate. The first set contained the 13 mm coverslip horizontally placed to mimic anaerobic condition, and the second set vertically to mimic aerobic condition. After overnight incubation at 37 °C, the coverslip was snapped into an appropriate size to mount onto 13 mm aluminium stubs. After washing the coverslip by PBS, the samples were fixed, rinsed, dehydrated, dried, and mounted. The argon was turned on and coating procedure was set up using the manual procedure for 120 s at 2.2 kV. At the end of coating procedure, samples were examined using a Hitachi S3000H Scanning Electron Microscope with an accelerating voltage of 10 kV.

3.1.1. Analysis of extracellular metabolites using milk broth medium

Milk assay was used to identify the types and amount of acids that are produced during growth of *K. pneumoniae* strains under different oxygen concentration. Two sets of inoculated 10 ml skimmed milk broth with 10^5 cells ml⁻¹ were incubated at 37 °C for 24 h on a shaker (200 rpm) for aerobic growth or in a static incubator for microaerobic growth. After incubation, samples were centrifuged at 4000 × g for 20 min, and the supernatant was analysed for lactate, acetate and formate production using commercial kits (Megazyme, Ireland). Amounts of organic acids produced by the different strains were expressed for 10⁸ CFU ml⁻¹.

3.1.2. Ethics statement

Mouse experiments at the University of Leicester were performed under the appropriate project (permit no. 60/4327) and personal (permit no. I66A9D84D) licenses according to the United Kingdom Home Office guidelines under the Animals Scientific Procedures Act 1986, and the University of Leicester ethics committee approval. The protocol was approved by both the UK Home Office and the University of Leicester ethics committee. Where indicated, the procedures were carried out under anaesthetic with isoflurane. Animals were housed in individually ventilated cages in a controlled environment and were frequently monitored after infection to minimize suffering. Every effort was made to minimize suffering and in bacterial infection experiments, mice were humanely culled if they became lethargic.

3.1.3. Colonization and chronic pneumonia model

To understand the importance of superoxide dismutase *in vivo* survival of *K. pneumoniae* KR3167, both colonization and chronic pneumonia models were utilized. Female 8–10 weeks old BALB/C mice weighing approximately 30–35 (Charles River, UK) were used. Mice had unlimited access to food and water throughout the experiment. The signs of infection (starry coat, hunched, lethargic) were monitored and recorded at regular intervals until the end of the experiment using well-established guidelines [37,38]. Prior to bacterial administration, mice were lightly anaesthetized with 3% v/v isoflurane and oxygen mixture (1.5–2 litre/min). Mice were intranasally administered with approximately 6×10^6 CFU per mouse in 20 µl sterile PBS for the colonization model, and 2×10^8 CFU per mouse in 50 µl for the chronic pneumonia model. To eliminate the possibility of secondary bacterial infection and

contamination during lung dissection another cohort was also inoculated as a control and received PBS alone. The mice were monitored periodically for the signs of disease. Then, for each time intervals, five mice were sacrificed, and the bacterial load in intranasal or lung tissue homogenates were measured by colony counting [39].

3.1.4. Statistical analysis

GraphPad Prism software version 6 (GraphPad, California, USA) was used for data analysis. The experimental results were expressed as mean ± standard error of the mean (SEM). Groups were compared by analysis of variance using One-way, Two-way ANOVA and Dunnett's multiple comparisons test. Less than 0.05 of *p*-value was regarded as statistically significant. Significance was defined as * *p* < 0.05, ** *p* < 0.01, *** *p* < 0.001 and **** *p* < 0.0001.

4. Results

4.1. The contribution of superoxide dismutases on aerobic growth and oxidative survival of *K. pneumoniae* KR3167

Under aerobic growth condition, the growth profiles of *K. pneumoniae* strains were determined in LB broth medium with or without 60 µM superoxide generator paraquat to evaluate the contribution of each *sod* in oxidative survival. Without paraquat the growth yield and rate of *sod* mutants were similar to that of wild type, except Δ *sodA::sodB* and Δ *sodA::sodB::sodC*, which had a significantly lower growth yield (Log₁₀ 8.82 ± 0.01 and 8.26 ± 0.02, respectively *n* = 3) and rate (2.41 h⁻¹ ± 0.04, and 1.35 h⁻¹ ± 0.03) than the wild type (growth yield: Log₁₀ 9.36 ± 0.01, growth rate: 3.21 h⁻¹ ± 0.02, *n* = 3) (*P* ≤ 0.0001) (Fig. 1A and B, and Supp. Fig. 1). When the severity of oxidative stress is increased by the addition of 60 µM paraquat, the growth yield and rate of Δ *sodA*, Δ *sodA::sodB*, Δ *sodA::sodC*, and Δ *sodA::sodB::sodC* were significantly lower than the wild type strain (*P* ≤ 0.0001) (Fig. 1C, D and Supp. Fig. 1). However, the growth yield and rate of Δ *sodB*, Δ *sodC*, and Δ *sodB::sodC* were not affected by paraquat relative to the wild type (*P* > 0.05). (Fig. 1C and D, and Supp. Fig. 1). These results show that under ambient oxygen concentration conditions, the microbe can tolerate the lack of single *sod* and the *sodA* codes for the most prominent SOD activity in *K. pneumoniae*.

In addition to LB, the M9 minimal medium was used because the high concentration of organic material in LB could mask the impact of an imposed oxidative stress. In M9-medium all mutant strains grew as well as the wild type except Δ *sodA::sodB* (Log₁₀ 6.72 ± 0.017 and 0.58 h⁻¹ ± 0.03, *n* = 3) and Δ *sodA::sodB::sodC* (Log₁₀ 6.79 ± 0.06 and 0.44 h⁻¹ ± 0.01, *n* = 3), which had lower growth yield and rate, respectively, than the wild type strain (growth yield: Log₁₀ 9.24 ± 0.02, and growth rate: 2.44 h⁻¹ ± 0.07, *n* = 3) (*P* ≤ 0.0001) (Fig. 1E, F, and Supp. Fig. 1). This observation suggests that *K. pneumoniae* can cope with the lack of a single *sod*, but cannot tolerate the absence of gene products for *sodA* and *sodB* together in the oxidative growth environment of M9-medium.

4.2. Effect of *sod* mutation on colony size

K. pneumoniae strains were assessed to evaluate the impact of SOD on colony size. The results on M9-agar showed that Δ *sodA::sodB* and Δ *sodA::sodB::sodC* mutants were unable to grow and form colonies, while Δ *sodA* and Δ *sodA::sodC* mutants had a significantly reduced colony size (0.71 mm ± 0.01 and 0.54 mm ± 0.01, *n* = 3, respectively), compared to the wild type (2.19 mm ± 0.02) (*P* ≤ 0.0001) (Supp. Fig. 2A). However, the genetically complemented mutants had a colony size significantly greater than their respective mutants (Supp. Figs. 2A and 2B). Moreover, no significant variations were found between wild type (1.38 mm ± 0.01) and Δ *sodB*; Δ *sodC*; and Δ *sodB::sodC* mutants (1.35 mm ± 0.01, 1.33 mm ± 0.02 and 1.31 mm ± 0.01, *n* = 3, respectively) (*P* > 0.05) (Supp. Fig. 2A).

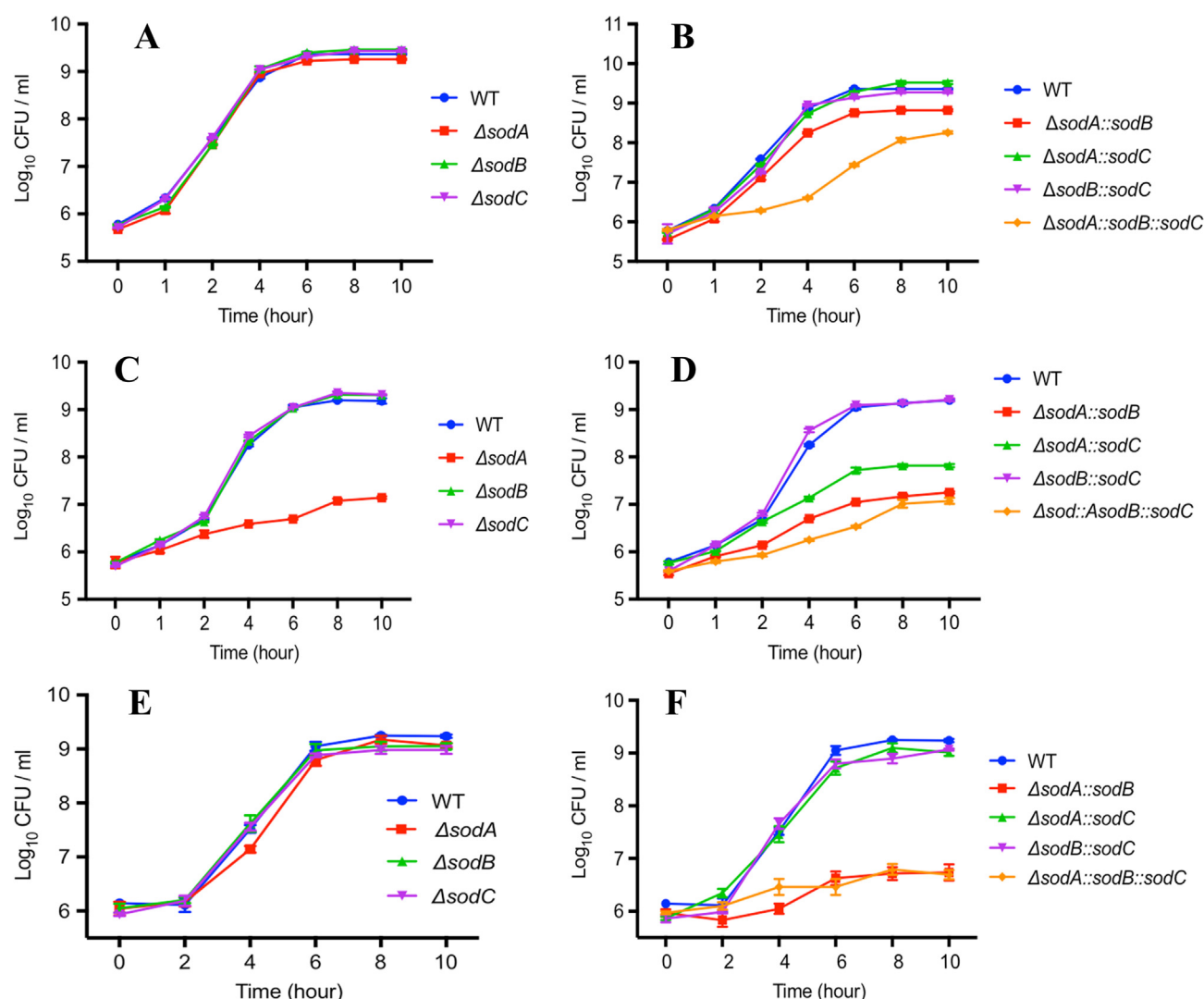


Fig. 1. Growth profiles of *K. pneumoniae* wild type and *sod* mutant strains under aerobic incubation. The growth profiles of the single (A and C) and double (B and D) mutants in LB broth medium, with (C and D) or without 60 μ M paraquat (A and B). The growth profiles of the single (E) and double (F) mutants in the minimal M9-broth medium. Each curve represents the mean of three experiments each in triplicate. Vertical bars represent the standard error of the mean.

On LB agar the colony sizes of the Δ sodA::sodB and Δ sodA::sodB::sodC mutants ($1.88 \text{ mm} \pm 0.04$ and $0.93 \text{ mm} \pm 0.03$, $n = 10$, respectively), were significantly smaller compared to the wild type strain ($2.19 \text{ mm} \pm 0.02$) ($P \leq 0.0001$) (Supp. Fig. 2B). However, no significant variations were noticed between colony size of wild type *K. pneumoniae* ($2.19 \text{ mm} \pm 0.02$), and the Δ sodA, and Δ sodA::sodC mutants ($2.01 \text{ mm} \pm 0.03$ and $2.13 \text{ mm} \pm 0.04$, $n = 3$, respectively) ($P > 0.05$) (Supp. Fig. 2B). Moreover, the sizes of Δ sodB, Δ sodC, and Δ sodB::sodC mutants on LB-agar appeared ($2.53 \text{ mm} \pm 0.04$, $2.49 \text{ mm} \pm 0.03$ and $2.38 \text{ mm} \pm 0.03$, $n = 3$, respectively) significantly larger than the wild type ($2.19 \text{ mm} \pm 0.02$) ($P \leq 0.0001$) (Supp. Fig. 2B). Therefore, it was concluded that expression of *sodA* has a key role in the maintenance of colony size on LB and M9-agar medium.

4.3. The impact of *sod* mutation on total superoxide dismutase activity

The total SOD activity of *K. pneumoniae* strains was determined as a percentage inhibition of chromogen reduction. In Δ sodA, Δ sodC, and Δ sodA::sodC the percentage inhibition was lower than Δ sodB, Δ sodA::sodB, Δ sodB::sodC, and wild type ($P \leq 0.0001$). However, as expected, no SOD activity could be recorded in triple Δ sodA::sodB::sodC mutant (Table 1). In conclusion, this result suggests that *sodB* is

Table 1

Characterization of SOD activity in the mutants, wild type *K. pneumoniae* KR3167 and its genetically complemented strains. Using SOD assay kit-WST, percentage inhibition of chromogen reduction was measured as an activity of SOD. The data is average of three independent experiments, each with triplicates. Error bars indicate standard error of the mean.

| Strains | % Inhibition |
|---------------------------|------------------|
| WT | 82.82 ± 0.80 |
| Δ sodA | 75.44 ± 0.11 |
| Δ sodB | 52.00 ± 0.58 |
| Δ sodC | 73.00 ± 0.58 |
| Δ sodA::sodB | 26.96 ± 0.46 |
| Δ sodA::sodC | 75.23 ± 0.72 |
| Δ sodB::sodC | 51.67 ± 0.88 |
| Δ sodA::sodB::sodC | 0.00 ± 0.00 |
| cis-sodA in Δ sodA | 85.27 ± 0.67 |
| cis-sodB in Δ sodB | 63.00 ± 0.58 |
| cis-sodC in Δ sodC | 81.37 ± 1.25 |

responsible for the major SOD activity of *K. pneumoniae*, followed in importance by the enzymes expressed by *sodA* and *sodC*. Consistent with the reduction in SOD activity, a reduction in H_2O_2 activity was observed in *sod* mutants, except in ΔsodC , relative to the wild type (Supp. Fig. 3).

4.4. Regulatory interactions among *sod* genes

We investigated regulatory interaction among different *sod* genes to determine whether a lack of one *sod* would be compensated by the increased expression of the other. As expected in triple mutant there was no detectable expression of either *sod* genes compared to the wild type (Supp. Table 4). The lack of *sodB* or *sodC* resulted in approximately two-fold up-regulation of *sodA* in ΔsodB , ΔsodC and $\Delta\text{sodB}::\text{sodC}$ (1.93 ± 0.02 -, 2.13 ± 0.02 - and 2.16 ± 0.02 -fold, $n = 3$, respectively) relative to the wild type (Supp. Table 4). Similarly, *sodC* expression was elevated in the absence of *sodA* and *sodB* in ΔsodA , ΔsodB and $\Delta\text{sodA}::\text{sodB}$ (2.60 ± 0.02 -, 2.08 ± 0.02 - and 3.75 ± 0.01 -fold, $n = 3$, respectively) (Supp. Table 4). However, *sodB* expression did not change (1.14 ± 0.01 , 1.26 ± 0.02 and 0.69 ± 0.05 , $n = 3$, respectively) in ΔsodA , ΔsodC , and $\Delta\text{sodA}::\text{sodC}$ relative to wild type (Supp. Table 4). The results indicated that both *sodA* and *sodC* are inducible, and compensate for the lack of other *sod* genes, whereas constitutive expression of *sodB* was not affected by the deletion of either *sodA* or *sodC*.

4.5. Impact of SOD activity on *K. pneumoniae* KR3167 metabolism

We hypothesised that in addition to oxidative stress resistance, SOD activity would have a major impact on metabolism, hence, the contribution of each SOD isozymes on *K. pneumoniae* metabolism was determined. Physical observations of milk broth coagulation indicated that aeration increased the coagulation. In aerobic growth, all mutants, except $\Delta\text{sodA}::\text{sodB}$ and $\Delta\text{sodB}::\text{sodC}$, showed coagulation in milk broth medium. However under microaerobic condition, milk coagulation was only noticed in ΔsodA , $\Delta\text{sodA}::\text{sodC}$, and $\Delta\text{sodA}::\text{sodB}::\text{sodC}$ (Fig. 2A and B).

Analysis of fermentation profiles under oxygenated growth showed that in wild type strain no lactate could be detected, and that the main fermentation end products were acetate and formate, whose origin was very likely from the acetate kinase/phospho-transacetylase and/or pyruvate-formate lyase pathways [40,41]. However, the absence of *sodA* significantly reduced the amount of acetate formation and led to lactate generation in ΔsodA , $\Delta\text{sodA}::\text{sodB}$, $\Delta\text{sodA}::\text{sodC}$ and $\Delta\text{sodA}::\text{sodB}::\text{sodC}$ in comparison to wild type, suggesting that the lack of *sodA* stimulates lactate dehydrogenase activity ($P \leq 0.0001$) (Fig. 2A).

Interestingly, expression of *sodC* resulted in acetate formation in ΔsodA and $\Delta\text{sodA}::\text{sodB}$ (1.30 ± 0.06 , 1.02 ± 0.06 g/L, $n = 3$, respectively) compared to the triple mutant $\Delta\text{sodA}::\text{sodB}::\text{sodC}$. However, expression of *sodB* did not affect the profile of metabolic end products in $\Delta\text{sodA}::\text{sodB}$ when compared to the triple mutant (Fig. 2A), indicating that *sodB* activity does not affect fermentation in the assay condition employed. It can be concluded that the formation of acetate indicates aerobic respiration that is due to the expression of *sodA* or *sodC*. However, the formation of both lactate and formate in the presence of *sodB* alone and in triple *sod* mutant suggest anaerobic respiration is occurring.

In microaerobic growth, the reduction of oxygen concentration was associated with varying levels of formate production in the mutants compared to wild type. The expression of *sodB* in $\Delta\text{sodA}::\text{sodC}$ did not affect the types of fermentative end products when compared to the triple mutant (Fig. 2B), while the expression of *sodA* led to a significant increase in acetate production in ΔsodB , ΔsodC and $\Delta\text{sodB}::\text{sodC}$ (1.76 ± 0.05 , 1.40 ± 0.04 , 1.69 ± 0.01 , $n = 3$, respectively) compared to the wild type (1.19 ± 0.06 , $n = 3$) ($P \leq 0.0001$) (Fig. 2B). Expression of *sodC* resulted in mixed acid fermentation in the ΔsodA

mutant (acetate: 0.41 ± 0.04 , lactate: 0.18 ± 0.01 , formate: 1.47 ± 0.01 , $n = 3$) and $\Delta\text{sodA}::\text{sodB}$ (acetate: 0.62 ± 0.05 , lactate: 0.24 ± 0.01 , formate: 0.30 ± 0.01 , $n = 3$) (Fig. 2B). Therefore, the changes in fermentation profiles were directly related to the expression of *sodA* and/or *sodC*. It can be concluded that expression of *sodA* determines acetate formation in both aerobic and microaerobic growth conditions, and its deletion is directly related to lactate formation in isogenic *sod* mutants. Moreover, *sodC* plays a metabolic role in acetate production. However, the expression of *sodB* does not affect fermentation end product formation.

4.6. Effect of *sod* deletion on β -galactosidase activity

It was reported that β -galactosidase activity is increased under oxidative stress in mammalian cells [26], but in *E. coli* the maximum β -galactosidase activity was detected in anaerobic rather than aerobic growth [42]. Therefore, it was hypothesised that there may be a relationship between SOD and β -galactosidase activity. The growth on LA supplemented with X-gal showed intensely blue coloured colonies, representing β -galactosidase activity, for $\Delta\text{sodA}::\text{sodB}$, $\Delta\text{sodA}::\text{sodC}$, and $\Delta\text{sodA}::\text{sodB}::\text{sodC}$ compared to the other mutants and wild type (Fig. 3A). However, the color intensity in ΔsodA , ΔsodB , ΔsodC , and $\Delta\text{sodB}::\text{sodC}$ was similar to the wild type (Fig. 3A). In addition, β -galactosidase activity was measured quantitatively in aerobic growth. Deletion of *sodA* alone or in combination with *sodB* or *sodC* led to a significant increase in β -galactosidase production in ΔsodA , $\Delta\text{sodA}::\text{sodB}$ and $\Delta\text{sodA}::\text{sodC}$. Moreover, in triple $\Delta\text{sodA}::\text{sodB}::\text{sodC}$ mutant a significant elevation of β -galactosidase production was observed (77.54 ± 4.15 U, $n = 3$) relative to wild type (2.89 ± 0.84 U, $n = 3$) ($P \leq 0.0001$) (Fig. 3B). However, β -galactosidase activity in ΔsodB , ΔsodC , and $\Delta\text{sodB}::\text{sodC}$ was similar to the wild type strain ($P > 0.05$) (Fig. 3B).

It can be concluded that the low level of β -galactosidase activity in wild type, ΔsodB , ΔsodC and $\Delta\text{sodB}::\text{sodC}$ directly related to the expression of *sodA*, which is linked to aerobic respiration. On the other hand, deletion of *sodA* alone or in combination with *sodB* and *sodC* significantly increased β -galactosidase activity. Therefore, the β -galactosidase activity might be useful as a biomarker to distinguish between aerobic and anaerobic respiration in Gram-negative Enterobacteriaceae.

4.7. The relationship between SOD expression and exopolysaccharide production

As SOD has a major influence on *K. pneumoniae* metabolism, we hypothesised that individual SOD isozymes would affect capsule synthesis differently. The results showed no significant difference in glucuronic acid levels between the wild type (60 ± 1 $\mu\text{g Log}_{10}$ 9 CFU $^{-1}$, $n = 3$) and ΔsodA , $\Delta\text{sodA}::\text{sodB}$, $\Delta\text{sodA}::\text{sodC}$, $\Delta\text{sodA}::\text{sodB}::\text{sodC}$ (43 ± 4 , 54 ± 1 , 59 ± 1 and 43 ± 5 $\mu\text{g Log}_{10}$ 9 CFU $^{-1}$, $n = 3$, respectively) ($P > 0.05$) (Fig. 4). On the other hand, ΔsodB , ΔsodC and $\Delta\text{sodB}::\text{sodC}$ had increased glucuronic acid production (89 ± 2 , 95 ± 2 and 87 ± 1 $\mu\text{g Log}_{10}$ 9 CFU $^{-1}$, $n = 3$, respectively) compared to the wild type ($P \leq 0.0001$) (Fig. 4). Together, these results suggested that there is an association between glucuronic acid content and the expression of *sodA*. Up-regulation of *sodA* in isogenic mutants, which is required for aerobic respiration, could increase the capsular polysaccharide production, which might then act as a barrier to minimize diffusion and intracellular level of oxygen.

4.8. Role of *sod* genes in biofilm formation

A previous study has indicated that cells encounter less oxygen within biofilms than during planktonic growth [43]. Therefore, the role of SOD activity in biofilm formation was investigated. The results showed that the ΔsodB , ΔsodC and $\Delta\text{sodB}::\text{sodC}$ mutants formed

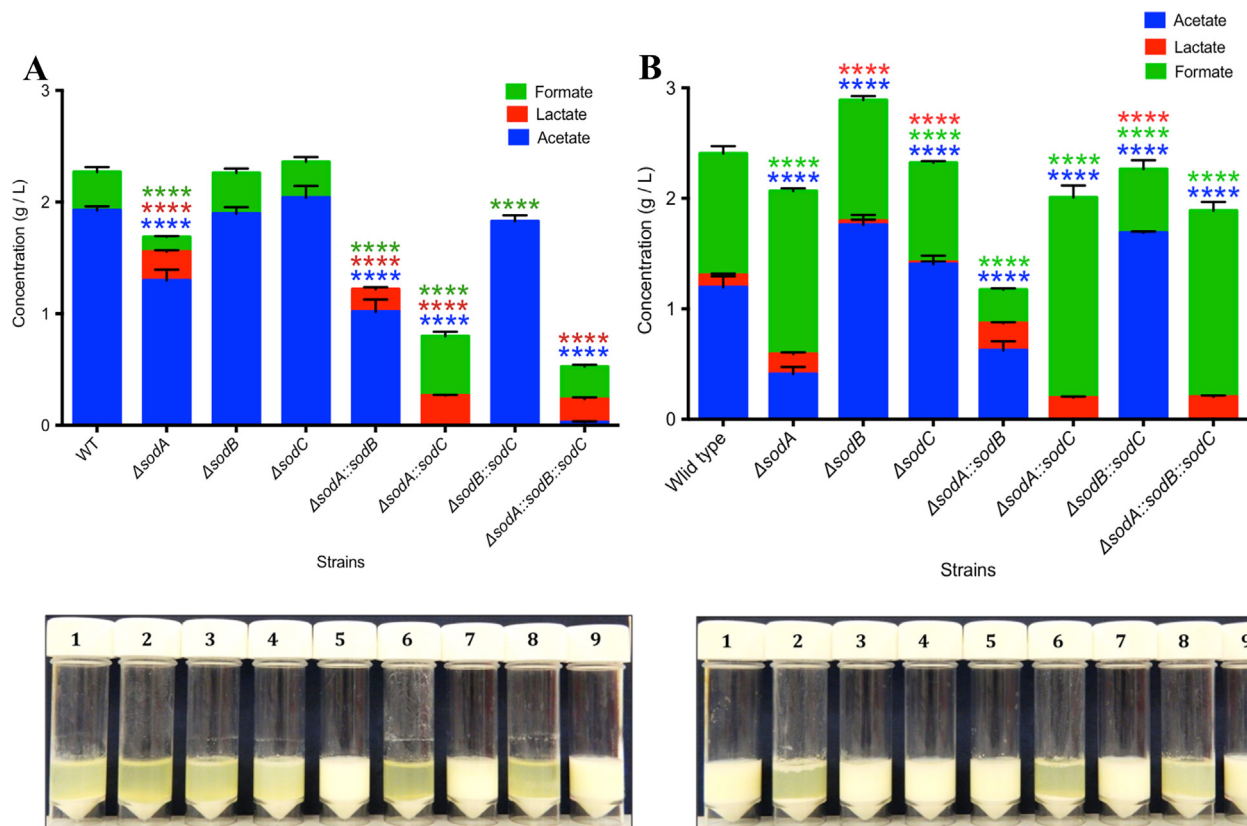


Fig. 2. Fermentation end product analysis of *K. pneumoniae* strains grown in 10% v/v skimmed milk at 37 °C for 24 h under aerobic (A) and microaerobic (B) growth condition. Each column represents means of three individual measurements each with triplicates with their standard error of means (vertical bars). Mean differences in fermentation profile of mutants were compared to the wild type strain using two-way ANOVA and Dunnett's multiple comparisons test (****P < 0.0001). Key: (1) Wild type, (2) Δ sodA, (3) Δ sodB, (4) Δ sodC, (5) Δ sodA::sodB, (6) Δ sodA::sodC, (7) Δ sodB::sodC, (8) Δ sodA::sodB::sodC, (9) Negative control, uninoculated medium.

significantly more biofilm than wild type (P < 0.0001), while Δ sodA, Δ sodA::sodB, Δ sodA::sodC and Δ sodA::sodB::sodC strains formed significantly less biofilm than wild type (P < 0.0001) (Fig. 5A). The overall trend in quantitative biofilm analysis showed that the presence of *sodA* enhanced biofilm formation, whereas, its deletion resulted in significant reduction. The difference in biofilm formation was not due to cell surface hydrophobicity of mutant strains as all strains had similar hydrophobicity, ranging between 76% and 80%. Similarly, no significant differences were seen in the numbers of planktonic cells of wild type or the mutants Δ sodB, Δ sodC and Δ sodB::sodC after 24 h incubation (P > 0.05) (Fig. 5B). However, biofilm former cells of Δ sodA, Δ sodA::sodC, Δ sodA::sodB and Δ sodA::sodB::sodC mutants were significantly lower than the wild type *K. pneumoniae* (P ≤ 0.0001) (Fig. 5B). These results suggest that difference in biofilm formation between mutants and wild type was not due to growth properties of strains.

The visual inspection of cultures showed that wild type, Δ sodB, Δ sodC and Δ sodB::sodC formed more biofilm at the top of the well where the oxygen concentration is expected to be higher, in comparison to Δ sodA, Δ sodA::sodB, Δ sodA::sodC and Δ sodA::sodB::sodC (Fig. 5C). Moreover, the wells containing Δ sodB, Δ sodC and Δ sodB::sodC had a ring-like red formazan deposition due to reduction in TCC, a sign of respiration, on the top biofilm strata, whereas, no ring formation could be detected for wild type, Δ sodA, Δ sodA::sodB, Δ sodA::sodC and Δ sodA::sodB::sodC strains (Fig. 5D). This shows that expression of *sodA* in mutant strains enhanced cell aggregation by minimizing the oxygen concentration within the biofilm communities, while its absence decreased the stress of aerobic respiration and reduced biofilm formation.

4.9. Microscopic analysis of *K. pneumoniae* biofilms

To investigate the SOD isozymes' role in biofilm architecture, mature biofilm structures on coverslips were analysed using a light microscope. The results showed substantial differences in the biofilm architecture of isogenic mutants compared with their wild type parent. The biofilm structure of the wild type is characterised by parallel lines, extending from the top to the bottom of the coverslip (Fig. 6A). However, the biofilm architecture of Δ sodA mutant contained branching aggregates, and the higher magnification revealed that these aggregates were somewhat linked (Fig. 6B). Interestingly, biofilm architecture of Δ sodB, Δ sodC and Δ sodB::sodC mutants contained massive cell aggregations on the top and web-like structure on the rest of coverslips (Fig. 6C, D and G). In biofilms of Δ sodA::sodB, Δ sodA::sodC and Δ sodA::sodB::sodC thin horizontal lines on the top and small patches of a cell aggregation on the bottom of coverslips, were observed (Fig. 6E, F and H). In general, the presence of *sodA* in mutant strains resulted in a web-like biofilm structure, and the appearance of such biofilms was distinguishable to the biofilms formed by wild type and other mutant strains that did not contain an intact copy of *sodA*.

Detailed analysis of the SOD's role in biofilm architecture and cell surface was carried out using SEM analysis. Fig. 7A shows the wild type biofilm in the form of a small group of a cell aggregation on coverslips, whereas the cells of Δ sodA (Fig. 7B) and Δ sodA::sodC (Fig. 7F) appeared to be slightly more elongated, and formed a biofilm of single cell attachment on coverslip surfaces. Interestingly, the Δ sodB, Δ sodC and Δ sodB::sodC strains formed compact cell aggregation and thick structure on coverslips, presumably space between cells were filled by polymeric matrix (Fig. 7C, -D and -G, respectively). In contrast, Δ sodA::sodB and Δ sodA::sodB::sodC (Fig. 7E and H, respectively) displayed a marked

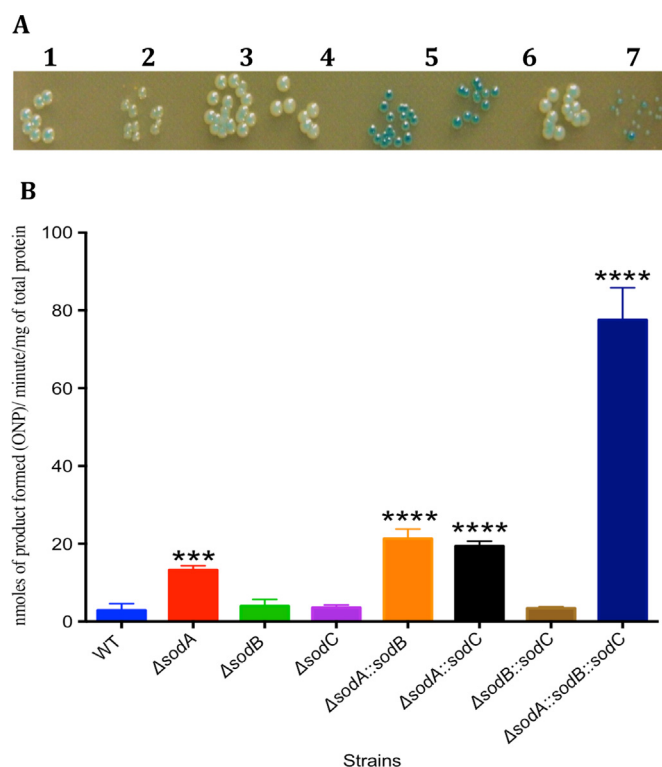


Fig. 3. Qualitative and quantitative β -galactosidase activity of *K. pneumoniae* strains. (A) Qualitative hydrolysis of X-Gal was analysed in isogenic mutants and wild type *K. pneumoniae* strains. Strains were grown under aerobic incubation at 37°C on LB agar plate supplemented with 1 μ g/ml of X-Gal (1) Wild type; (2) Δ sodA; (3) Δ sodB; (4) Δ sodC; (5) Δ sodA::sodB; (6) Δ sodA::sodC; (7) Δ sodB::sodC and (8) Δ sodA::sodB::sodC. (B) Quantitative measurement of β -galactosidase activity in *K. pneumoniae* strains. Each column represents the average of three independent experiments, each with triplicates. Error bars indicate standard error of the mean. One-way ANOVA and Dunnett's multiple tests were used for comparison *** $P \leq 0.0001$, compared to wild type.

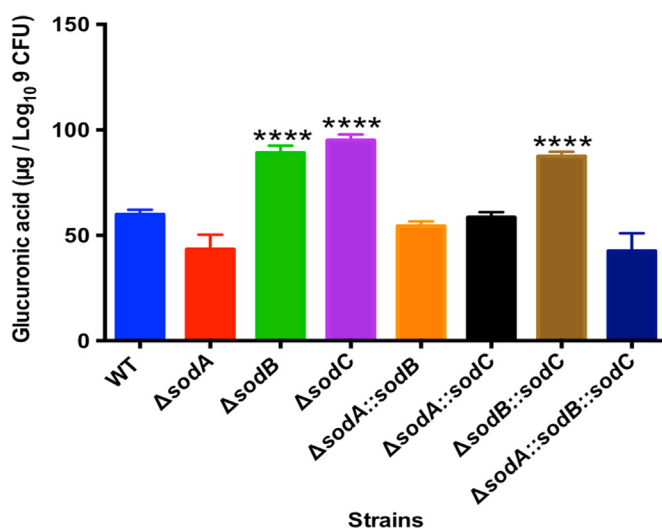


Fig. 4. Glucuronic acid quantification in *K. pneumoniae* sod strains. From overnight microaerobic cultures, equivalent numbers of cells were used for quantification of glucuronic acid concentration. Glucuronic acid concentration of capsular polysaccharide was quantified using carbazole assay and expressed as μ g Log₁₀ 1 $\times 10^9$ CFU⁻¹. Data are means of three independent experiments each in triplicates. P-value was determined by one-way ANOVA and Dunnett's multiple comparisons test relative to wild type (**** $P \leq 0.0001$).

reduction in cell aggregation compared to wild type, and the mutant cells varied in size and were significantly elongated in comparison to wild type (Fig. 7A).

Furthermore, in order to investigate the SOD isozymes role in cell size and biofilm architecture in an oxygenated environment, biofilms were initiated on coverslips that were placed vertically to allow 2/3 of the coverslip to be within the medium and 1/3 out of the medium for full exposure to atmospheric oxygen. The results showed noticeable differences in biofilm architecture and cell morphology between the mutants and wild type strain in an oxygenated environment. Wild type cells appeared equal in size with wrinkled surface surrounded by exopolysaccharide matrix and with several cellular projection and curli filaments, which provide interconnection between the cells and mediate adherence to the substratum (Fig. 8A). In contrast, Δ sodA (Fig. 8B), Δ sodA::sodB Δ sodA::sodC (Fig. 8E and F, respectively), and Δ sodA::sodB::sodC (Fig. 8H) displayed clear differences in comparison to the wild type strain, in that the cells were more elongated and individually attached to the coverslip surface with the absence of interconnecting projections between the cells. Interestingly, the cells of Δ sodB, Δ sodC (Fig. 8C and D) and Δ sodB::sodC (Fig. 8G) exhibited massive cell aggregation on top of coverslips, which had been exposed to oxygen. The bacteria had a wrinkled surface and were densely packed with an indistinguishable outline of biofilm layer.

Under anaerobic condition, wild type cells were surrounded by capsular polysaccharide and interconnected through finger-like projections that extended from cell to cell and to the surface substratum (Fig. 9A). In contrast, Δ sodA (Fig. 9B) cells were sparsely distributed and were interconnected by a fine filament-like polymeric matrix, Δ sodB (Fig. 9C), Δ sodC (Fig. 9D) while Δ sodB::sodC (Fig. 9G) maintained a densely packed structure. Cells closely adhered through cellular projections covered by the substantial polymeric matrix. Δ sodA::sodB and Δ sodA::sodC exhibited elongation and morphological changes, and the cells were arranged as chains or scattered individually on the surface (Fig. 9E and F). On the other hand, Δ sodA::sodB::sodC showed unique morphological feature as these cells were covered with a pocket like rigid capsular polysaccharide (Fig. 9H). These results show that oxygen concentration gives rise to different cell morphologies and aggregation properties, which are influenced by the presence or absence of *sodA* in *K. pneumoniae*. Hence, SOD activity is important not only for the elimination of superoxide radical in aerobic growth but also has a role in the anaerobic condition.

4.10. Role of *sod* genes in the survival of *K. pneumoniae* KR3167 in nasopharyngeal tissue

As the nasopharynx is a highly oxygenated environment, the contribution of SOD isozymes on *K. pneumoniae* survival in nasopharynx was analysed after intranasal infection. The bacterial counts showed no significant difference among different groups immediately after infection, illustrating the accuracy and consistency of inoculation ($P > 0.05$) (Fig. 10A). The numbers of wild type and mutant strains decreased progressively 12-h post infection, and with the exception of double Δ sodA::sodB and triple Δ sodA::sodB::sodC mutants no significant reduction was noticed between wild type and other mutants, which might be related to the slow growth rate of Δ sodA::sodB and Δ sodA::sodB::sodC. However, at 24 h post infection, the results showed that Δ sodA, Δ sodA::sodB, Δ sodA::sodC and Δ sodA::sodB::sodC mutant strains had decreased in numbers in nasopharyngeal tissue compared to the wild type ($P \leq 0.05$) (Fig. 10A), while Δ sodB, Δ sodC, and Δ sodB::sodC numbers were similar to that of wild type ($p > 0.05$) (Fig. 10A). Overall, it can be concluded that *sodA* alone or in combination with *sodB* and *sodC* contributes to *K. pneumoniae* survival in nasopharynx but that *sodB* and *sodC* do not.

In addition, the SODs role in chronic lung infection model was also investigated. It was found that no bacteria could be detected in the blood during the course of infection, neither in wild type nor in mutant-

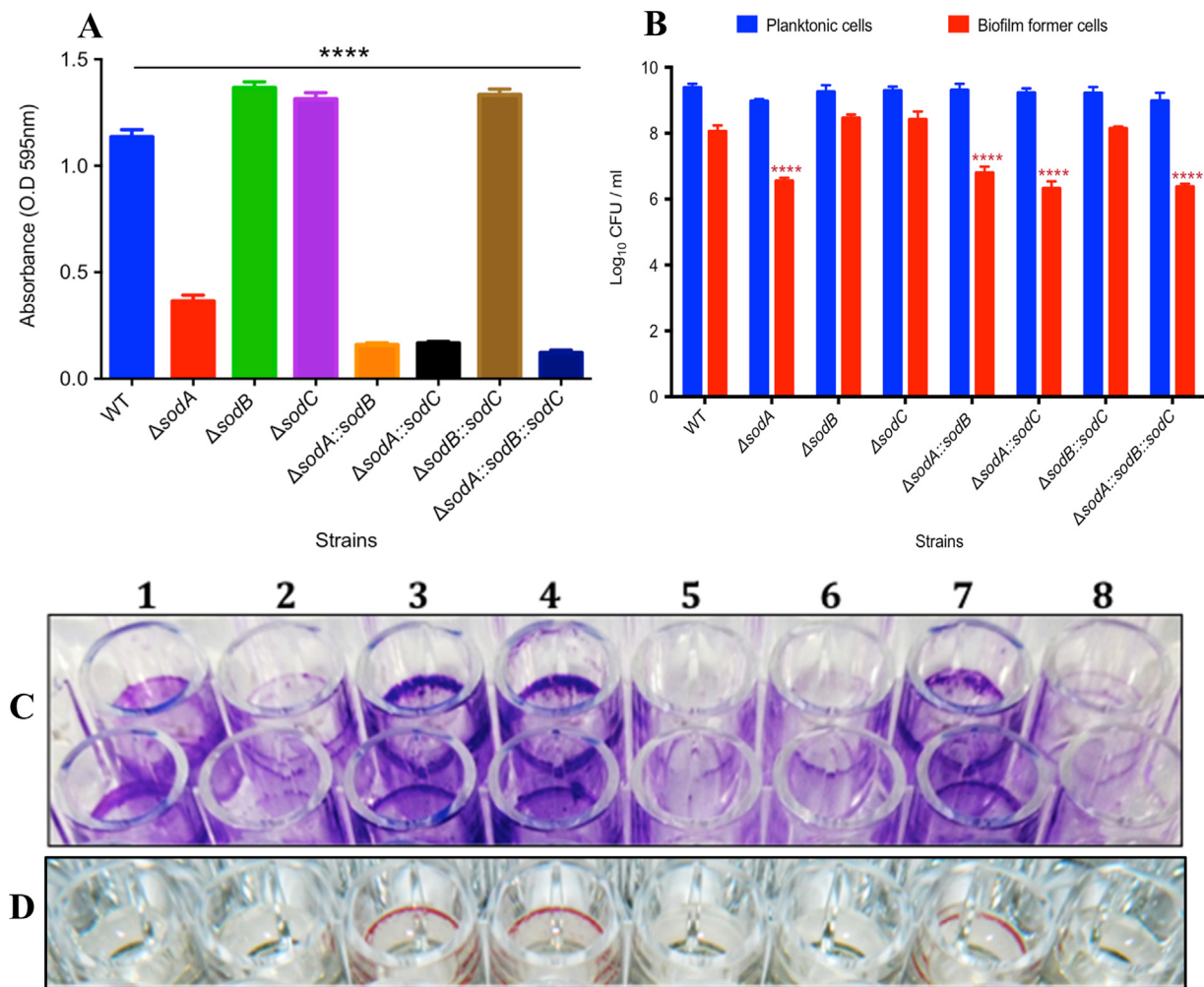


Fig. 5. Analysis of SODs role in *K. pneumoniae* biofilm formation. **(A and C)** Evaluation of biofilm formation of *K. pneumoniae* strains by crystal violet staining method. The strains were grown in LB in microaerobic condition in a 96-well polystyrene microplate for 24 h. **(B)** The viable counts for planktonic and biofilm former cells. Planktonic cells were removed and quantified by colony counting. **(D)** Biofilms were stained with 0.02% (w/v) trimethyl tetrazolium chloride (TTC). (1) Wild type (2) $\Delta sodA$ (3) $\Delta sodB$ (4) $\Delta sodC$ (5) $\Delta sodA::sodB$; (6) $\Delta sodA::sodC$ (7) $\Delta sodB::sodC$ (8) $\Delta sodA::sodB::sodC$. Data represent the mean \pm SEM of four independent experiments, each with triplicates. Values are means four independent experiments of triplicates using ANOVA and Dunnett's multiple comparisons tests (****P < 0.0001).

infected mouse cohorts. Hence, this model allowed us to ideally determine SOD isozyme contribution to *K. pneumoniae* survival in the oxygenated environment of the lungs. Immediately after infection viable counts of lung tissue homogenates were found to be similar for different cohorts. However, four days post-infection, the bacterial load in the lungs significantly decreased in comparison to initial bacterial numbers for all cohorts (Fig. 10B). However, the highest reduction was seen in mice infected with $\Delta sodA::sodB$, and $\Delta sodA::sodB::sodC$ (Log_{10} 0.85 ± 0.12 , 0.57 ± 0.05 , and 0.08 ± 0.08 , mg^{-1} tissue, $n = 5$, respectively) compared to the wild type (Log_{10} 1.55 ± 0.14 , mg^{-1} tissue, $n = 5$) ($P \leq 0.0001$) (Fig. 10B). Moreover, after 17-days post-infection, a significant reduction in numbers of $\Delta sodA$, $\Delta sodC$ and complete clearance of $\Delta sodB::sodC$, $\Delta sodA::sodC$, and $\Delta sodA::sodB::sodC$ were observed. However, $\Delta sodA$, $\Delta sodC$ and $\Delta sodA::sodB$ (Log_{10} 0.41 ± 0.32 , 0.08 ± 0.08 and 0.68 ± 0.08 , mg^{-1} tissue, $n = 5$, respectively) persisted in the lung tissue. It can be concluded that different SODs have different roles in the survival of *K. pneumoniae* in the lungs. In the early phase, up to 4 days post-infection, it appeared that both *sodA* and *sodB* are required for survival of *K. pneumoniae* in the lower respiratory tract. In the late phase, up to 17 days post-infection, the presence of *sodC* apparently determines the persistence of *K. pneumoniae* in the lungs as $\Delta sodA::sodB$ mutant resisted clearance.

5. Discussion

The removal of superoxide radicals must be vital for microbes exposed to aerobic life, which is evident from the multiplicity of SOD isozymes in bacterial species. Although all three known SOD isozymes in bacteria catalyse the same reaction, it is not known whether there are functional differences nor the regulatory interactions among SODs. In this study, we used a unique experimental setting to answer these questions by creating single, double, and triple SOD mutants in *K. pneumoniae*. Our results showed that there are functional differences among SOD isozymes, and their role is not limited to removal of superoxide and growth in an oxygenated environment but that SOD activity influences microbial metabolism, biofilm formation and architecture, β -galactosidase activity, and survival in oxygenated animal tissues.

Aerobic growth of $\Delta sodB$, $\Delta sodC$, and $\Delta sodB::sodC$ mutants in LB alone, LB with paraquat, and M9-medium indicate that inducible Mn-SOD enables a major protection against oxidative stress, which provides a growth advantage to *K. pneumoniae*. This is very likely because of the accumulation of $\text{O}_2^{\cdot-}$ increases oxidation of Mn^{+2} to Mn^{+3} , which in turn competes with Fe^{+2} for metal binding sites of apo SOD [44]. In response to aerobic challenge *sodA* is overexpressed in $\Delta sodB$, $\Delta sodC$

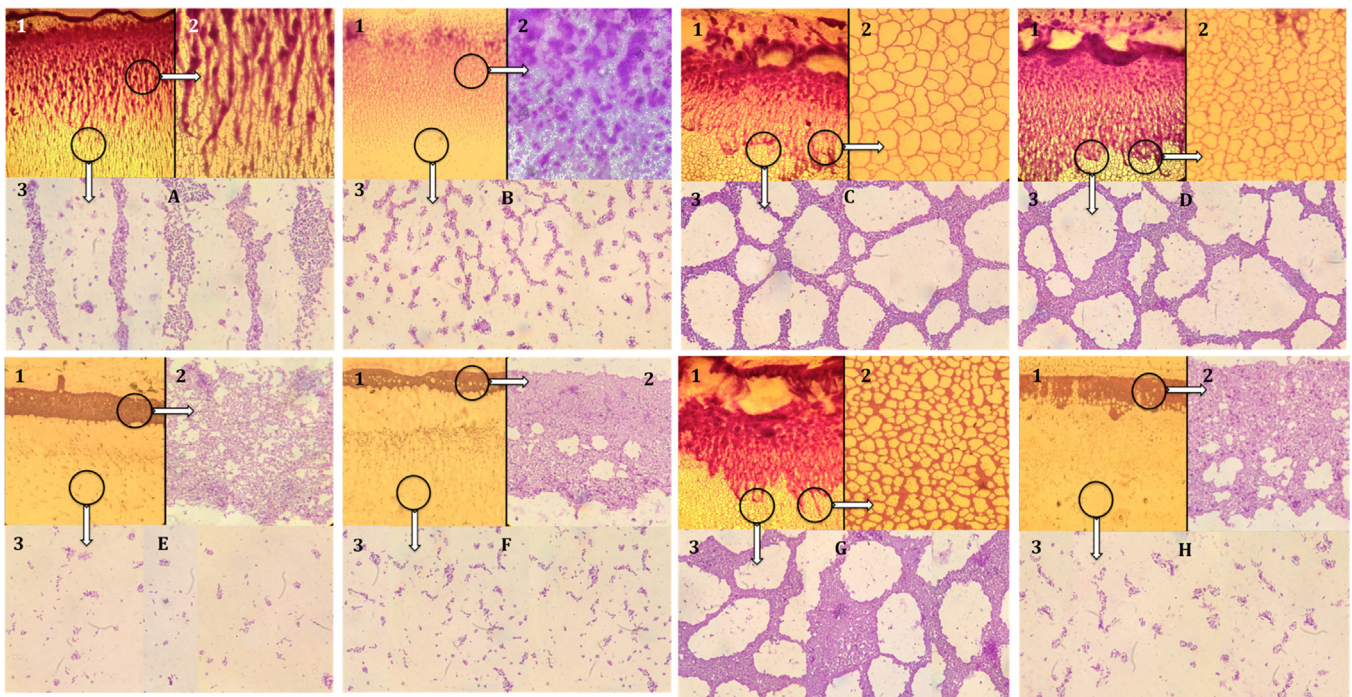


Fig. 6. Light microscopic analysis of biofilm formation and architecture of *K. pneumoniae* strains. SOD mutants and wild type strains of *K. pneumoniae* were inoculated into fresh Luria-Bertani broth in equivalent numbers and distributed into 12-well polystyrene plates containing vertically positioned coverslips. The cultures were incubated under the microaerobic condition at 37 °C for 24 hrs. Then, the coverslips were removed, passed through PBS, stained with 1% (w/v) crystal violet for 1 min, and the excess stain was removed by passing through PBS. Representative biofilm images for (A) wild type, (B) Δ sodA, (C) Δ sodB, (D) Δ sodC, (E) Δ sodA::sodB, (F) Δ sodA::sodC, (G) Δ sodB::sodC, and (H) Δ sodA::sodB::sodC. (1) under 100 \times magnification, (2) under 600 \times magnification, (3) under 1000 \times magnification. This experiment was repeated three times to confirm the reproducibility.

and Δ sodB::sodC, to remove the increased intracellular level of $O_2^{\cdot-}$. Also, deletion of *sodB* might have caused an imbalance in iron homeostasis. Dubrac and Touati (2000) emphasised that deficiency in environmental iron concentration causes *E. coli* to reduce production of iron-containing proteins, and the shortage of Fe-SOD is compensated by

induction of Mn-SOD [45]. While the expression of *sodA* went up in an oxygenated environment, the total SOD enzymatic activity in mutants did not profoundly increase. It could therefore be possible that insufficient availability of intracellular manganese as a cofactor might be responsible for this observation.

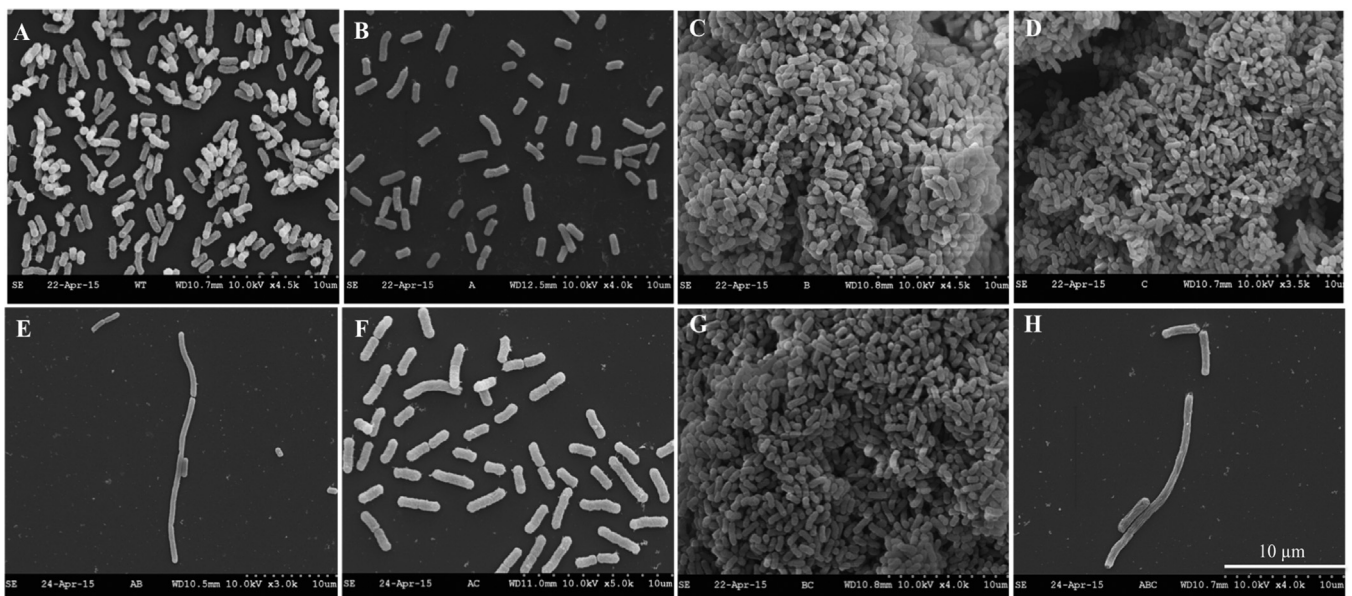


Fig. 7. SEM analysis of biofilm ultrastructure and cell morphology of *K. pneumoniae* strains in microaerobic growth. The panels shown are at 10 μ m resolution. Cover slides were vertically placed into 12-well plates, inoculated with mutants or wild type *K. pneumoniae*, and incubated for 24 h at 37 °C under microaerobic condition. Coverslips were removed and processed for scanning electron microscopy. Micrographs are showing different biofilm morphology: (A) shows microcolonies of wild type *K. pneumoniae*, (B) Δ sodA, (C) Δ sodB, (D) Δ sodC (E) Δ sodA::sodB, (F) Δ sodA::sodC, (G) Δ sodB::sodC (H) Δ sodA::sodB::sodC. SEMs of cultures were examined under 10 kV power and 10 μ m magnification. Representative images from 3 independent experiments, and for each image 5 fields were examined.

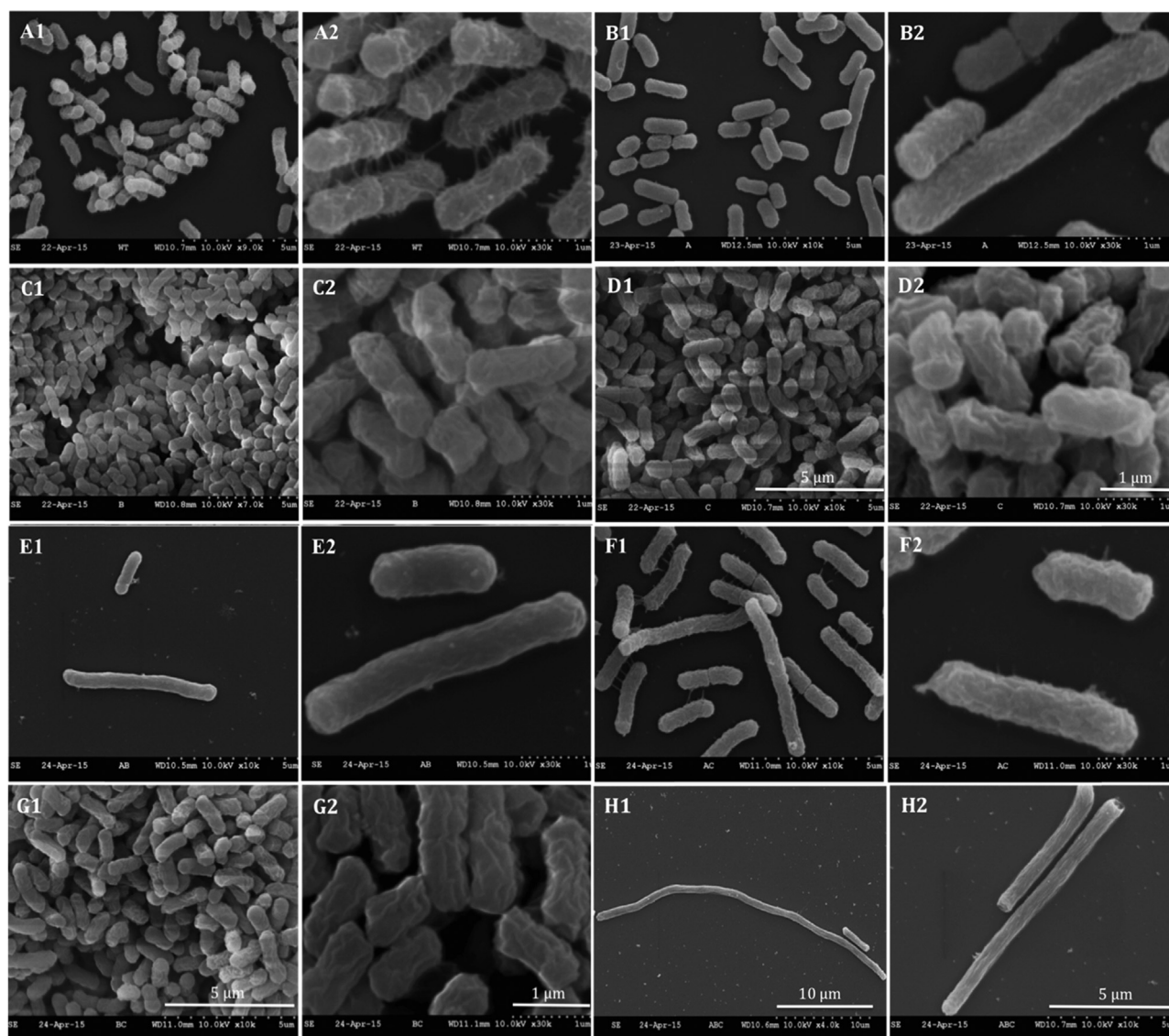


Fig. 8. Scanning electron micrographs of biofilm formed by *K. pneumoniae* strains in microaerobic condition. Most of the cells attached to the top part of a vertically placed coverslip. A1 and A2 represent wild type cells with interconnecting finger-like projections, likely composed of exo-polysaccharide; B1 and B2 show a group of isogenic $\Delta sodA$ cells with smooth surfaces; C1 and C2 are for $\Delta sodB$, and D1 and D2 are for $\Delta sodC$, both with wrinkled cell surface, massively stacked without finger-like projections between the cells. F1 and F2 are for $\Delta sodA::sodC$, with slightly elongated cells with a wrinkled surface, and interconnected by finger-like projections. G1 and G2 are for $\Delta sodB::sodC$, cells appeared with wrinkled surface, massively stacked without an interconnection between the cells. H1 and H2 are for $\Delta sodA::sodB::sodC$, the cells appeared with variable size and smooth surface but without interconnection between the cells. A1, B1, C1, D1, E1, F1, G1, and H1 indicates low magnification (5 μm), and A2, B2, C2, D2, E2, F2, G2, and H2 show high magnification (1 μm). Representative images from three independent experiments, and for each image 5 fields were examined.

The results of this report indicate that up-regulation of *sodA* enhances aerobic respiration, leading to maximum production of O_2^{2-} [46]. This increase in ROS might have an adverse effect on other oxygen labile enzymes and intracellular molecules. Therefore, metabolic adaptation can occur in response to ROS toxicity. In *Burkholderia cenocepacia* several metabolic pathways differ in their response to high ROS levels [47]. In this study we found high acetate production under both aerobic and microaerobic conditions due to metabolic alterations in $\Delta sodB$, $\Delta sodC$, and $\Delta sodB::sodC$ mutants. Bettenbrock *et al.* (2014) showed that *E. coli* in highly oxygenated condition convert a large amount of sugar to acetate via the acetate kinase/phospho-transacetylase pathway [40]. It is therefore reasonable to assume that maximum acetate production acts as a defence mechanism to reduce superoxide efflux from the TCA cycle.

Surprisingly, deletion of *sodA* under highly oxygenated growth condition lead to increase in β -galactosidase activity in $\Delta sodA$,

$\Delta sodA::sodC$, $\Delta sodA::sodB$ and $\Delta sod::sodB::sodC$ mutants. In these mutants, aerobiosis increases β -galactosidase activity due to the lack of *sodA*, which means that these mutants switch to anaerobic fermentation mode (as described in fermentation profile above). However, previous studies have showed that under anaerobic incubation conditions (increase in CO_2) *E. coli* increases β -galactosidase activity [42]. In our experimental setting, the lack of *sodA* in mutant *K. pneumoniae* strains automatically turned the metabolic pathway to anaerobic fermentation without a need for an increase in CO_2 pressure or anaerobic incubation. This could be due to an accumulation of signal molecules indicating stress, such as adenosine 3',5'-cyclic monophosphate (cAMP), guanosine 3',5'-bispyrophosphate (ppGpp) or catabolite activator protein (CAP). These signals were reported to increase under anaerobic growth condition, which in turn reduce bacterial growth rate and stimulate *lacZ* gene expression [42,48].

Our results suggest that inducible *sodA* does not only protect the *K.*

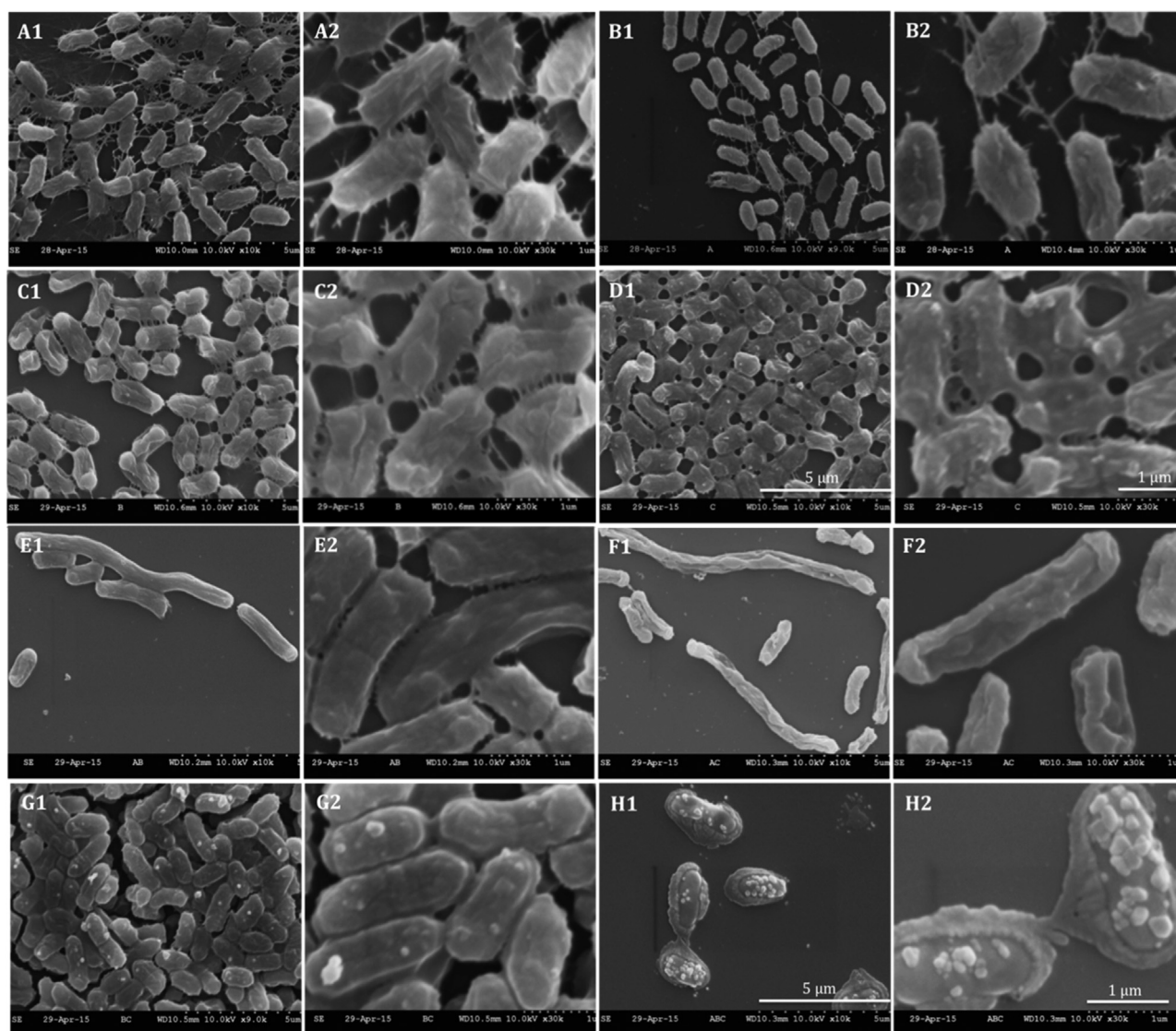


Fig. 9. Scanning electron micrographs of biofilm formed by isogenic mutants and wild type *K. pneumoniae* under anaerobic culture conditions. Panels A1 and A2 show the micrographs of the wild type strain. The surface of the coverslip was colonized with a layer of bacterial cells embedded in exopolysaccharide and interconnected with a finger-like projection of exopolysaccharide matrix. B1 and B2 are showing $\Delta sodA$ cells with their interconnecting fine filaments, C1 and C2 are for $\Delta sodB$, and D1 and D2 are for $\Delta sodC$. For both strains, the cells were close to each other, and were interconnected with short fine filament-like structure with a massive exopolysaccharide matrix. E1 and E2 show isogenic $\Delta sodA::sodB$, slightly elongated cells with a smooth surface and interconnected with short filament-like structure, F1, F2 represent isogenic $\Delta sodA::sodC$ mutant, slightly elongated chain of cells with the folded cell surface, interconnected by single polar projections. G1, G2 isogenic $\Delta sodB::sodC$ mutant. Cells are stacked compactly and embedded within wax like an exopolysaccharide matrix. H1, H2 are isogenic $\Delta sodA::sodB::sodC$ mutant. Cells are scattered and embedded in a pocket-like rigid exo-polysaccharide structure. A1, B1, C1, D1, E1, F1, G1, and H1 indicates low magnification (5 μm), and A2, B2, C2, D2, E2, F2, G2, and H2 show high magnification (1 μm). Representative images from three independent experiments are shown. For each image 5 fields were examined.

pneumoniae cell from the toxicity of $O_2^{\cdot -}$, but also its activity regulates other genes involved in exopolysaccharide (EPS) production, and biofilm formation on the abiotic surface. High EPS production and biofilm formation in *K. pneumoniae* $\Delta sodB$, $\Delta sodC$, $\Delta sodB::sodC$ mutants could be part of a protective mechanism to minimize direct cell exposure and permeability of oxygen to the cell, which in turn equilibrate oxygen uptake and $O_2^{\cdot -}$ formation from aerobic respiration. Kim et al. highlighted that interstitial channels of biofilm structure reduce cells' exposure to oxygen [49]. EPS production linked to biofilm formation in some bacteria as an adaptive response against general stress [50], such as in *Bradyrhizobium japonicum* [51], and *Acinetobacter oleivorans* [52]. In these bacteria, $O_2^{\cdot -}$ and H_2O_2 stress resulted in high-level EPS production and biofilm formation.

Analysis of the metabolic activity of mutants in undisrupted biofilm showed that $\Delta sodB$, $\Delta sodC$ and $\Delta sodB::sodC$ are able to reduce soluble

colourless TTC to an intracellular red insoluble triphenylformazan (TPF) dye, very likely due to the intact Mn-SOD activity in these strains. The ability to reduce tetrazolium dye can be linked to low levels of oxygen in cellular biomass or to active aerobic respiration. Prigent-Combaret et al. demonstrated that cells within a biofilm encounter more limited oxygen than planktonic cells [43]. High EPS production and extensive cell aggregation with highly active rates of metabolism could be the reason for the low intracellular level of oxygen and quick red deposition of insoluble formazan observed in the $\Delta sodB$, $\Delta sodC$, and $\Delta sodB::sodC$ mutants.

The detailed mechanisms of alterations in biofilm architecture and massive cell aggregation in $\Delta sodB$, $\Delta sodC$, $\Delta sodB::sodC$ mutants currently are unclear. However, it could be speculated that biofilm architecture and cell arrangement of *K. pneumoniae* is significantly influenced by oxygen, and by the activity of Mn-SOD. Under aerobic

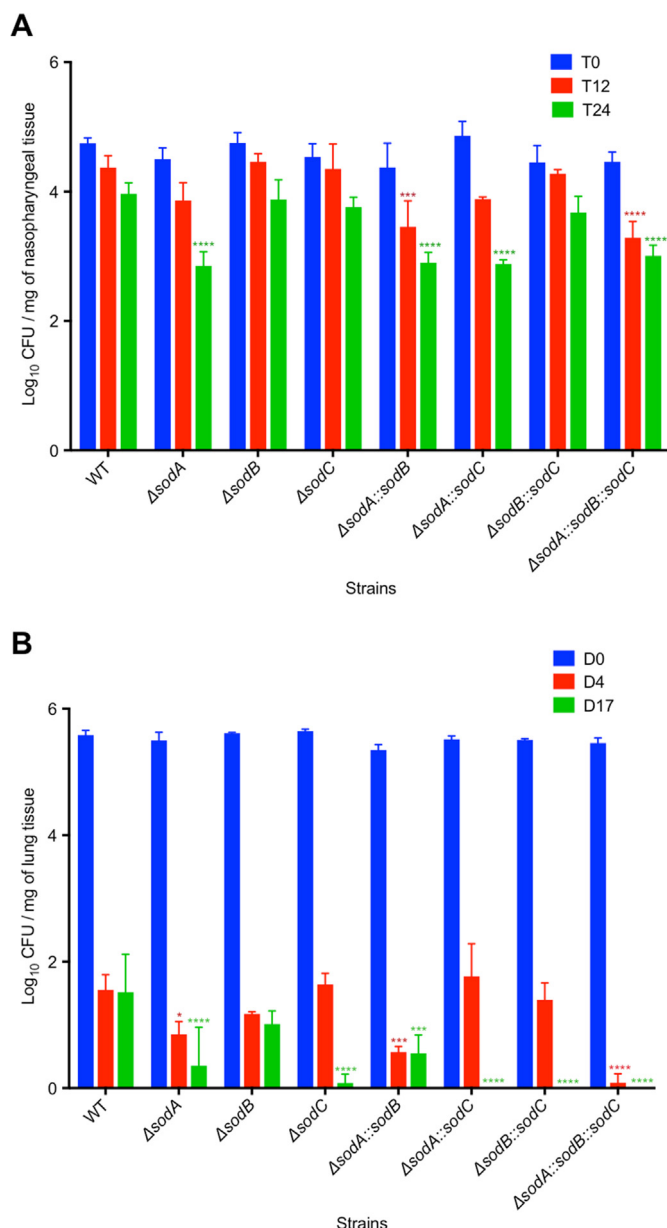


Fig. 10. Survival of *K. pneumoniae* *sod* mutant strains in nasopharyngeal (A) and lung tissues of BALB/c mice. (A) Eight weeks old female BALB/c mice were inoculated intranasally with approximately 6×10^6 CFU/mouse in 20 μ l of PBS. Bacterial load (Log_{10} CFU mg^{-1}) was determined at predetermined time points in nasopharyngeal tissue homogenates. T0: time zero of inoculation, T12:12 h post infection, T24:24 h post infection. (B) Bacterial counts of mutants and wild type *K. pneumoniae* in lung tissues were determined at different time intervals. Eight weeks old female BALB/c mice were inoculated intranasally with 50 μ l of PBS containing between 2×10^8 to 2.5×10^8 CFU/mouse. Bacterial load (Log_{10} CFU mg^{-1}) was determined in homogenized lung tissue. D0: immediately after infection, D4: 4 days post-infection, D17:17 days post-infection. In (A) and (B) each column represents the mean Log_{10} CFU mg^{-1} derived from five mice and the bars represent the standard error of the mean. Two-way ANOVA and Dunnett's multiple comparisons test were used for analysis **** $P \leq 0.0001$ relative to wild type counts for the same time point.

attachment, the probability of aerobic respiration and endogenous $\text{O}_2^{\cdot-}$ formation in ΔsodB , ΔsodC , $\Delta\text{sodB}::\text{sodC}$ mutants are much higher than anaerobic attachment. Therefore, alteration in biofilm architecture might occur in response to redox balance, which is important for cellular function, and survival.

Growth attenuation of the $\Delta\text{sodA}::\text{sodC}$ mutant under superoxide

stress shows that constitutive expression of *sodB* alone is not enough to provide protection against $\text{O}_2^{\cdot-}$ toxicity. Moreover, constitutive expression of *sodB* has no impact on the fermentation profile under either aerobic or microaerobic conditions. Shrivastav et al. showed that *K. pneumoniae* under anaerobic conditions enhances the synthesis of lactate dehydrogenase, pyruvate-formate lyase, and α -acetolactate synthase, which are used to convert pyruvate into lactate, formate, and 2,3-butanediol, respectively [41]. Pyruvate formate-lyase (PFL) is critical for the survival of facultative anaerobic bacteria in low oxygen environments, and acts as a central metabolic enzyme containing an oxygen-labile $[4\text{Fe-4S}]^+$ cluster, therefore, its expression is 12–15-times higher in *E. coli* under anaerobic than aerobic conditions [53]. Furthermore, it has been reported that lactate dehydrogenase (LDH) inactivated by hydroxyl radical [54]. It is very likely that the amount of formate and lactate increased with a reduction in oxygen levels in microaerobic condition.

Periplasmic Cu/Zn-SOD accounts for only 2% of the total SOD activity in *E. coli* and it is believed to be important for protection against exogenously produced superoxide [12]. For *K. pneumoniae* the absence of a single or both cytosolic SODs stimulates the expression of *sodC* in the ΔsodA , ΔsodB , and $\Delta\text{sodA}::\text{sodB}$ mutants. The increase in *sodC* expression in these mutant backgrounds clearly shows the SodC contribution to cytoplasmic clearance of superoxide. However, we cannot rule out the possibility that increase in *sodC* expression may be due to other metabolic imbalances in the ΔsodA , ΔsodB , and $\Delta\text{sodA}::\text{sodB}$ mutants. The presence of *sodC* affected *K. pneumoniae* SOD activity and provided a growth advantage and increased bacterial colony size to double in the $\Delta\text{sodA}::\text{sodB}$ mutant compared to the triple $\Delta\text{sodA}::\text{sodB}::\text{sodC}$ mutant. Metabolic analysis revealed that the role of *sodC* is not only restricted to periplasmic protection from exogenous $\text{O}_2^{\cdot-}$ but also it is involved in mixed acid fermentation pathways.

In vivo results obtained in this study showed that the numbers of wild type and mutant strains decreased progressively 12- and 24 h post infection. Reduction in the numbers of mutant strains in our colonization model of infection reflects the impact of *sodA* deletion on the growth of *K. pneumoniae* under oxygenated condition. In addition to colonization, a chronic respiratory infection model was also established in BALB/c mice to demonstrate the role of SODs in *K. pneumoniae* KR3167 survival. Four days post pulmonary infection, the bacterial load of the *K. pneumoniae* $\Delta\text{sodA}::\text{sodB}$, and $\Delta\text{sodA}::\text{sodB}::\text{sodC}$ mutants was significantly reduced when compared to wild type *K. pneumoniae* KR3167. Interestingly, after 17-days post-infection significant reduction in growth of ΔsodA , ΔsodC and complete clearance of $\Delta\text{sodB}::\text{sodC}$, $\Delta\text{sodA}::\text{sodC}$, and $\Delta\text{sodA}::\text{sodB}::\text{sodC}$ mutants were observed. It is therefore likely that the gradual decrease of bacterial counts after 4 days, and complete clearance of most mutants after 17 days post-infection can be linked to the partial pressure of oxygen and lung immune responses. Significant reduction in the ΔsodC count, and the maintenance of the $\Delta\text{sodA}::\text{sodB}$ mutant in the lungs of BALB/c mice strongly supports the view that the activity of periplasmic Cu/Zn-SOD is required for *K. pneumoniae* chronic lung infection by fending off the ROS produced by macrophages or for scavenging of periplasmic $\text{O}_2^{\cdot-}$ generated during stationary phase of endogenous metabolism [55].

Our results provide the first evidence showing the involvement of Cu/Zn-SOD in wider metabolic pathways and in filament formation of *K. pneumoniae*. Ultrastructural analysis of biofilms attributed an additional role for *sodC* in filamentous morphology of $\Delta\text{sodA}::\text{sodB}$ mutant under both microaerobic and anaerobic conditions. It is possible to speculate that filaments provide additional protection against phagocytosis during chronic pneumonia. The metabolic analysis of *sod* mutants showed that expression of *sodC* in $\Delta\text{sodA}::\text{sodB}$ mutant induces a unique metabolic profile that is different from that in wild type and the triple $\Delta\text{sodA}::\text{sodB}::\text{sodC}$ mutant. Therefore, it is reasonable to assume that the filamentous appearance of $\Delta\text{sodA}::\text{sodB}$ mutant arose due to alterations in metabolism.

In summary, our study has shown that different SOD isozymes in *K.*

pneumoniae have unique roles in the removal of superoxide radical, that there is an interplay among SOD isozymes. We have shown that SOD function is not limited to removal of superoxide radicals but extends to metabolic reprogramming, biofilm and capsule synthesis, cell morphology, as well as nasopharyngeal colonization and persistence in chronic lung infection. Our findings will lead to a shift in the conceptual understanding of microbial oxidative stress resistance, and SODs role in this process. In future, we plan to investigate system level response of the bacterial cell to superoxide toxicity.

Appendix A. Supporting information

Supplementary data associated with this article can be found in the online version at doi:10.1016/j.freeradbiomed.2019.01.018.

References

- [1] R.A. Miller, B.E. Britigan, Role of oxidants in microbial pathophysiology, *Clin. Microbiol. Rev.* 10 (1997) 1–18.
- [2] E. Cabiscol, J. Tamarit, J. Ros, Oxidative stress in bacteria and protein damage by reactive oxygen species, *Int. Microbiol.* 3 (2000) 3–8.
- [3] K.L. Seib, H.J. Wu, S.P. Kidd, M.A. Apicella, M.P. Jennings, A.G. McEwan, Defenses against oxidative stress in *Neisseria gonorrhoeae*: a system tailored for a challenging environment, *Microbiol. Mol. Biol. Rev.* 70 (2006) 344–361.
- [4] B.J. Sheehan, P.R. Langford, A.N. Rycroft, S.J. Kroll, [Cu, Zn]-Superoxide dismutase mutants of the swine pathogen *Actinobacillus pleuropneumoniae* are unattenuated in infections of the natural host, *Infect. Immun.* 68 (2000) 4778–4781.
- [5] A. Carliz, D. Touati, Isolation of superoxide-dismutase mutants in *Escherichia coli* - is superoxide dismutase necessary for aerobic life, *EMBO J.* 5 (1986) 623–630.
- [6] L. Benov, I. Fridovich, Functional significance of the Cu, ZnSOD in *Escherichia coli*, *Arch. Biochem. Biophys.* 327 (1996) 249–253.
- [7] S.B. Farr, R.D. Ari, D. Touati, Oxygen-dependent mutagenesis in *Escherichia coli* lacking superoxide dismutase, *PNAS* 83 (1986) 8268–8272.
- [8] A.J. Case, On the origin of superoxide dismutase: an evolutionary perspective of superoxide-mediated redox signaling, *Antioxidants* 6 (2017) 1–21.
- [9] G. Porcheron, A. Garénaux, J. Proulx, M. Sabri, C.M. Dozois, Iron, copper, zinc, and manganese transport and regulation in pathogenic enterobacteria: correlations between strains, site of infection and the relative importance of the different metal transport systems for virulence, *Front. Cell Infect. Microbiol.* 3 (2013) 1–24.
- [10] A.S. Gort, D.M. Ferber, J.A. Imlay, The regulation and role of the periplasmic copper, zinc superoxide dismutase of *Escherichia coli*, *Mol. Microbiol.* 32 (1999) 179–191.
- [11] A.B. Sadosky, J.W. Wilson, H.M. Steinman, H.A. Shuman, The iron superoxide dismutase of *Legionella pneumophila* is essential for viability, *J. Bacteriol.* 176 (1994) 3790–3799.
- [12] S.G. John, H.M. Steinman, Periplasmic copper-zinc superoxide dismutase of *Legionella pneumophila*: role in stationary-phase survival, *J. Bacteriol.* 178 (1996) (1587–84).
- [13] I. Fridovich, Superoxide radical: an endogenous toxicant, *Annu. Rev. Pharmacol. Toxicol.* 23 (1983) 239–257.
- [14] E.C. Niederhoffer, C.M. Naranjo, K.L. Bradley, J.A. Fee, Control of *Escherichia coli* superoxide dismutase (SodA and SodB) genes by the ferric uptake regulation (*fur*) locus, *J. Bacteriol.* 172 (1990) 1930–1938.
- [15] R.A. D'Mello, P.R. Langford, J.S. Kroll, Role of bacterial Mn-cofactored superoxide dismutase in oxidative stress responses, nasopharyngeal colonization, and sustained bacteremia caused by *Haemophilus influenzae* type b, *Infect. Immun.* 65 (1997) 2700–2706.
- [16] P. Armshaw, J.T. Pembroke, Generation and analysis of an ice r391 deletion library identifies genes involved in the element encoded uv-inducible cell-sensitising function, *FEMS Microbiol. Lett.* 342 (2013) 45–53.
- [17] T.T. Hoang, R.R. Karkhoff-Schweizer, A.J. Kutchma, H.P. Schweizer, A broad-host-range *ftp-frt* recombination system for site-specific excision of chromosomally-located DNA sequences: application for isolation of unmarked *Pseudomonas aeruginosa* mutants, *Gene* 212 (2013) 77–86.
- [18] J.J. van Aartsen, K. Rajakumar, An optimized method for suicide vector-based allelic exchange in *Klebsiella pneumoniae*, *J. Microbiol. Methods* 86 (2011) 313–319.
- [19] A.A. Miles, S.S. Misra, J.O. Irwin, The estimation of the bactericidal power of the blood, *J. Hygiene* 38 (1938) 732–749.
- [20] B. Lesic, L.G. Rahme, Use of the lambda red recombinase system to rapidly generate mutants in *Pseudomonas aeruginosa*, *BMC Mol. Biol.* 9 (2008) 20.
- [21] M.K. Chaveroche, J.M. Ghigo, C. D'Enfert, A rapid method for efficient gene replacement in the filamentous fungus *Aspergillus nidulans*, *Nucleic Acids Res.* 28 (2000) e97.
- [22] F.A.Y. Al-Bayati, H.F.H. Kahya, A. Damianou, S. Shafeeq, O.P. Kuipers, P.W. Andrew, H. Yesilkaya, Pneumococcal galactose catabolism is controlled by multiple regulators acting on pyruvate formate lyase, *Sci. Rep.* 7 (2017) 43587.
- [23] P. Gaspar, F.A.Y. Al-Bayati, P.W. Andrew, A.R. Neves, H. Yesilkaya, Lactate dehydrogenase is the key enzyme for pneumococcal pyruvate metabolism and pneumococcal survival in blood, *Infect. Immun.* 82 (2014) 5099–5109.
- [24] X. Zhi, I.T. Abdullah, O. Gazioglu, I. Manzoor, S. Shafeeq, O.P. Kuipers, N.L. Hiller, P.W. Andrew, H. Yesilkaya, Rgg-Shp regulators are important for pneumococcal colonization and invasion through their effect on mannose utilization and capsule synthesis, *Sci. Rep.* 8 (2018) 6369.
- [25] K.J. Livak, T.D. Schmittgen, Analysis of relative gene expression data using real-time quantitative PCR and the 2(-delta delta c(t)) method, *Methods* 25 (2001) 402–408.
- [26] F. Debacq-Chainiaux, J.D. Erusalimsky, J. Campisi, O. Toussaint, Protocols to detect senescence-associated beta-galactosidase (SA-beta-gal) activity, a biomarker of senescent cells in culture and *in vivo*, *Nat. Protoc.* 4 (2009) 1798–1806.
- [27] X. Zhang, H. Bremer, Control of the *Escherichia coli* *rrnBp1* promoter strength by ppGpp, *J. Biol. Chem.* 270 (1995) 11181–11189.
- [28] S. Cho, J. Law, C. Ng, Effect of growth at sub-lethal concentrations of kanamycin on the cell membrane integrity and amount of capsular glucuronic acid in wild type *Escherichia coli* and strain with a *cpsB* mutation, *J. Exp. Microbiol. Immunol.* 13 (2009) 29–35.
- [29] S. Favre-Bonte, B. Joly, C. Forestier, Consequences of reduction of *Klebsiella pneumoniae* capsule expression on interactions of this bacterium with epithelial cells, *Infect. Immun.* 67 (1999) 554–561.
- [30] M.D.S. Goncalves, C. Delattre, D. Balestrino, N. Charbonnel, R. Elboutachfai, A. Wadouchi, S. Badel, T. Bernardi, P. Michaud, C. Forestier, Anti-biofilm activity: a function of *Klebsiella pneumoniae* capsular polysaccharide, *PLoS One* 9 (2014) e99995.
- [31] Y.C. Lai, H.L. Peng, H.Y. Chang, RmpA2, an activator of capsule biosynthesis in *Klebsiella pneumoniae* CG43, regulates K2 *cps* gene expression at the transcriptional level, *J. Bacteriol.* 185 (2003) 788–800.
- [32] Y. Suo, Y. Huang, Y. Liu, C. Shi, X. Shi, The expression of superoxide dismutase (SOD) and a putative ABC transporter permease is inversely correlated during biofilm formation in *Listeria monocytogenes* 4b G, *PLoS One* 7 (2012) e48467.
- [33] H. Xu, H.Y. Lee, J. Ahn, Growth and virulence properties of biofilm-forming *Salmonella enterica* serovar Typhimurium under different acidic conditions, *Appl. Environ. Microbiol.* 76 (2010) 7910–7917.
- [34] L.M. Pérez, B.L. Alvarez, F. Codony, M. Fittipaldi, B. Adrados, G. Peñuela, J. Morató, A new microtitre plate screening method for evaluating the viability of aerobic respiring bacteria in high surface biofilms, *Lett. Appl. Microbiol.* 51 (2010) 331–337.
- [35] K. Shukho, K. Mi, K. Hee, S. Sung, C. Dong, K. Jungmin, A simple colorimetric method for testing antimicrobial susceptibility of biofilmed bacteria, *J. Microbiol.* 48 (2010) 709–711.
- [36] M. Rosenberg, D. Gutnick, E. Rosenberg, Adherence of bacteria to hydrocarbons - a simple method for measuring cell-surface hydrophobicity, *FEMS Microbiol. Lett.* 9 (1980) 29–33.
- [37] D.B. Morton, P.H.M. Griffiths, Guidelines on the recognition of pain, distress & discomfort in experimental animals & an hypothesis for assessment, *Vet. Rec.* 116 (1985) 431–436.
- [38] A. Motib, A. Guerreiro, F. Al-Bayati, E. Piletska, I. Manzoor, S. Shafeeq, A. Kadam, O. Kuipers, L. Hiller, T. Cowen, S. Piletsky, P.W. Andrew, H. Yesilkaya, Modulation of quorum sensing in a Gram-positive pathogen by linear molecularly imprinted polymers with anti-infective properties, *Angew. Chem. Int. Ed. Engl.* 56 (2017) 16555–16558.
- [39] A. Kadam, R.A. Eutsey, J. Rosch, X. Miao, M. Longwell, W. Xu, C.A. Woolford, T. Hillman, A.S. Motib, H. Yesilkaya, A.P. Mitchell, N.L. Hiller, Promiscuous signaling by a regulatory system unique to the pandemic PMEN1 pneumococcal lineage, *PLoS Pathog.* 13 (2017) e1006339.
- [40] K. Bettenbrock, H. Bai, M. Ederer, J. Green, K.J. Hellingwerf, M. Holcombe, S. Kunz, M.D. Rolfe, G. Sanguinetti, O. Sawodny, P. Sharma, S. Steinsiek, R.K. Poole, Towards a systems level understanding of the oxygen response of *Escherichia coli*, *Adv. Microb. Physiol.* 64 (2014) 65–114.
- [41] A. Shrivastav, J. Lee, H.Y. Kim, Y.R. Kim, Recent insights in the removal of Klebsiella pathogenicity factors for the industrial production of 2,3-butanediol, *J. Microbiol. Biotechnol.* 23 (2013) 885–896.
- [42] B.I.N. Lin, A. Wang, N. Cheng, Impact of carbon dioxide gas and carbonate ions on the growth of *Escherichia coli* K-12 b23 and on the induced -galactosidase activity: exploring models for global regulation, *JEMI* 1 (2001) 19–31.
- [43] C. Prigent-Combaret, O. Vidal, C. Dorel, P. Lejeune, Abiotic surface sensing and biofilm-dependent regulation of gene expression in *Escherichia coli*, *J. Bacteriol.* 181 (1999) 5993–6002.
- [44] S.Y. Pugh, I. Fridovich, Induction of superoxide dismutases in *Escherichia coli* B by metal chelators, *J. Bacteriol.* 162 (1985) 196–202.
- [45] S. Dubrac, D. Touati, Fur positive regulation of iron superoxide dismutase in *Escherichia coli*: functional analysis of the *sodB* promoter, *J. Bacteriol.* 182 (2000) 3802–3808.
- [46] J.A. Imlay, the molecular mechanisms and physiological consequences of oxidative stress: lessons from a model bacterium, *Nat. Rev. Microbiol.* 11 (2013) 443–454.
- [47] E. Peeters, A. Sass, E. Mahenthiralingam, H. Nelis, T. Coenye, Transcriptional response of *Burkholderia cenocepacia* J2315 sessile cells to treatments with high doses of hydrogen peroxide and sodium hypochlorite, *BMC Genom.* 11 (2010) 90.
- [48] J.H. Lee, W.J. Dobrogosz, Effects of aerobic and anaerobic shock on catabolite repression in cyclic amp suppressor mutants of *Escherichia coli*, *J. Bacteriol.* 154 (1983) 992–994.
- [49] Y.H. Kim, Y. Lee, S. Kim, J. Yeom, S. Yeom, B. Seok Kim, S. Oh, S. Park, C.O. Jeon, W. Park, The role of periplasmic antioxidant enzymes (superoxide dismutase and thiol peroxidase) of the shiga toxin-producing *Escherichia coli* O157:H7 in the formation of biofilms, *Proteomics* 6 (2006) 6181–6193.
- [50] P. Landini, Cross-talk mechanisms in biofilm formation and responses to environmental and physiological stress in *Escherichia coli*, *Res. Microbiol.* 160 (2009) 259–266.

- [51] A.J. Donati, J.M. Jeon, D. Sangurdekar, J.S. So, W.S. Chang, Genome-wide transcriptional and physiological responses of *Bradyrhizobium japonicum* to paraquat-mediated oxidative stress, *Appl. Environ. Microbiol.* 77 (2011) 3633–3643.
- [52] I.A. Jang, J. Kim, W. Park, Endogenous hydrogen peroxide increases biofilm formation by inducing exopolysaccharide production in *Acinetobacter oleivorans* Dr1, *Sci. Rep.* 6 (2016) 1–12.
- [53] J. Yang, S.G. Naik, D.O. Ortillo, R. García-Serres, M. Li, W.E. Broderick, B. Huynh, J.B. Broderick, The iron- sulfur cluster of pyruvate formate-lyase activating enzyme in whole cells: cluster interconversion and a valence-localized [4Fe-4S] 2+ state, *Biochemistry* 48 (2009) 9234–9241.
- [54] J.D. Buchanan, D.A. Armstrong, Free radical inactivation of lactate dehydrogenase, *Int. J. Radiat. Biol. Relat. Stud. Phys. Chem. Med.* 30 (1976) 115–127.
- [55] R. Gabbianelli, C. Signoretti, I. Marta, A. Battistoni, L. Nicolini, *Vibrio cholerae* periplasmic superoxide dismutase: isolation of the gene and overexpression of the protein, *J. Biotechnol.* 109 (2004) 123–130.